

A Joint Time-Invariant Filtering Approach to the Linear Gaussian Relay Problem

Cheulsoon Kim, *Student Member, IEEE*, Youngchul Sung[†], *Senior Member, IEEE*, and
Yong H. Lee, *Senior Member, IEEE*

Abstract

In this paper, the linear Gaussian relay problem is considered. Under the linear time-invariant (LTI) model the problem is formulated in the frequency domain based on the Toeplitz distribution theorem. Under the further assumption of realizable input spectra, the LTI Gaussian relay problem is converted to a joint design problem of source and relay filters under two power constraints: one at the source and the other at the relay, and a practical solution to this problem is proposed based on the projected subgradient method. Numerical results show that the proposed method yields a noticeable gain over the instantaneous amplify-and-forward (AF) scheme in inter-symbol interference (ISI) channels. Also, the optimality of the AF scheme within the class of one-tap relay filters is established in flat-fading channels.

Keywords

Linear Gaussian relay, linear time-invariant model, Toeplitz distribution theorem, projected subgradient method, filter design

[†]Corresponding author

The authors are with the Dept. of Electrical Engineering, KAIST, Daejeon 305-701, South Korea. E-mail: {lghid@stein., ysung@ee. and yohlee@}kaist.ac.kr. This work was supported in part by the IT R & D program of MKE/KEIT [2008-F-004-02, “5G mobile communication systems based on beam division multiple access and relays with group cooperation”]. This research was also supported in part by the KCC (Korea Communications Commission), Korea, under the R & D program supervised by the KCA (Korea Communications Agency) (KCA-2011-11913-04001).

I. INTRODUCTION

Relay networks have drawn extensive interest from research communities because they play an important role in enlarging the network coverage in wireless communications. Although the capacity of relay networks is not exactly known yet, many ingenious coding strategies including decode-and-forward (DF), compress-and-forward (CF), etc. beyond simple AF schemes have been developed [1, 2]. Recently, Zahedi et al. proposed an advanced linear scheme for relay networks based on (strictly-)causal linear processing at the relay to compromise the complexity and performance between the complicated coding strategies and the simple AF* scheme [3, 4]. While information theorists approached the problem from the perspective of capacity and capacity-achieving schemes [5–8], researchers in the signal-processing community also tackled this problem based on measures like the received signal-to-noise ratio (SNR) or minimum mean square error (MMSE). Most of their results are based on the setup in which linear processing is at the relay and destination but not at the source, e.g., [9, 10]. Although these works provide meaningful approaches to the relay problem, it is not optimal not to have processing at the source from the fundamental perspective of data-rate maximization. To this end the processing at the source such as the input covariance function design should be incorporated together with the processing at the relay. (Once the processing at the source and relay is fixed, the optimal destination processing is automatically given for several well-known criteria.) However, the joint design of source and relay processing is a hard problem even in the linear Gaussian case, as shown in [3, 4]. In [3, 4], the authors considered general time-varying linear processing at the relay in Gaussian channels. Although they obtained the capacity for frequency-division strictly-causal linear relaying, the general linear relay case was not explored fully [3, 4]. In the general linear relay case, the problem is a sequence of non-convex optimization problems, and it is seemingly intractable. To circumvent such difficulty, in this paper we consider tractable and practical LTI filtering at the source and relay. We find that it is still a hard problem to obtain the capacity with a single-letter characterization even in this case because the search space still has countably infinite dimensions; optimal source and relay filters may have infinite impulse responses (IIRs). However, we *provide a practical solution to design the source and relay filters jointly to maximize the transmission rate for general ISI Gaussian relay networks.*

Under the LTI framework, the linear Gaussian relay problem can be formulated in the frequency domain using the Toeplitz distribution theorem [11, 12]. When the relay filter is given and there is no power

*In this paper, the AF scheme means the instantaneous AF scheme, which can easily be implemented by simple analog processing.

constraint on the relay, the problem reduces to the classical ISI channel problem for which the optimal strategy is known as water-filling in the frequency domain [13, pp. 407 - 430]. However, the freedom to design the relay filter and the power constraint at the relay make the problem far more difficult than the classical ISI channel problem, especially when stability and causality constraints are imposed on the source and relay filters. Our approach to this problem is that we first convert the problem to a *constrained optimization problem in a finite dimensional space* by restricting the source and relay filters to the class of finite impulse response (FIR) filters as in most practical filtering applications, and then apply the *projected subgradient method*, initially proposed by Polyak [14] and fully developed by Yamada et al. [15, 16], to this problem. Numerical results show that our method performs well and yields a noticeable gain over the AF scheme in ISI relay channels.

Notations and Organizations

We will make use of standard notational conventions. Vectors and matrices are written in boldface with matrices in capitals. All vectors are column vectors. For a scalar a , a^* denotes its complex conjugate. For a matrix \mathbf{A} , \mathbf{A}^T , \mathbf{A}^H and $\text{tr}(\mathbf{A})$ indicate the transpose, Hermitian transpose and trace of \mathbf{A} , respectively, and $\mathbf{A}(m, n)$ denotes the m -th row and n -th column element of \mathbf{A} . $\text{diag}(d_1, \dots, d_n)$ denotes a diagonal matrix with elements d_1, \dots, d_n . \mathbf{I}_n stands for the identity matrix of size n (the subscript is omitted when unnecessary), and $\mathbf{0}$ denotes a vector of all zero elements. For a vector \mathbf{a} , $\|\mathbf{a}\|$ denotes its 2-norm. The notation $\mathbf{x} \sim \mathcal{N}(\boldsymbol{\mu}, \boldsymbol{\Sigma})$ means that \mathbf{x} is Gaussian-distributed with mean vector $\boldsymbol{\mu}$ and covariance matrix $\boldsymbol{\Sigma}$. $\mathbb{E}\{\cdot\}$ denotes the expectation. For two signal processes $x[n]$ and $y[n]$, $x[n] * y[n]$ denotes the convolution of the two processes. \mathbb{R} , \mathbb{I} , \mathbb{I}_+ and \mathbb{N} denote the sets of real numbers, integers, nonnegative integers and natural numbers, respectively. For two sets A and B , $A \setminus B$ denotes the set minus operation. $j = \sqrt{-1}$.

This paper is organized as follows. The system model and background are described in Section II. In Section III, the rate formula in the frequency domain is derived under the LTI model, and the performance of LTI relaying in flat-fading channels is investigated in Section IV. In Section V, a joint source and relay filter design method is proposed based on the projected subgradient method, and its performance in ISI channels is examined in Section VI, followed by conclusions in Section VII.

II. SYSTEM MODEL AND BACKGROUND

We consider the general discrete-time additive white Gaussian noise (AWGN) relay network composed of source, relay and destination nodes, as shown in Fig. 1, where the source and relay nodes have maxi-

mum available average power P_s and P_r , respectively. We assume that all propagation channels (i.e., the source-to-relay (S-R), relay-to-destination (R-D) and source-to-destination (S-D) channels) are linear, time-invariant and causal, and their impulse responses are absolutely summable, i.e., $\sum_{l=0}^{\infty} |h_{sr}[l]| < \infty$, $\sum_{l=0}^{\infty} |h_{rd}[l]| < \infty$ and $\sum_{l=0}^{\infty} |h_{sd}[l]| < \infty$, where $h_{sr}[l]$, $h_{rd}[l]$ and $h_{sd}[l]$ are the S-R, R-D and S-D channel impulse responses, respectively. Due to the absolute summability, the z -transforms of the propagation channel impulse responses are well-defined and given by $H_{sr}(z) = \sum_{l=0}^{\infty} h_{sr}[l]z^{-l}$, $H_{rd}(z) = \sum_{l=0}^{\infty} h_{rd}[l]z^{-l}$ and $H_{sd}(z) = \sum_{l=0}^{\infty} h_{sd}[l]z^{-l}$. Then, the received signals at the relay and destination at the n -th symbol time are given by

$$y_r[n] = h_{sr}[n] * x_s[n] + w_r[n], \quad \text{and} \quad (1)$$

$$y_d[n] = h_{sd}[n] * x_s[n] + h_{rd}[n] * x_r[n] + w_d[n], \quad (2)$$

respectively, where $x_s[n]$ is the transmitted signal process at the source; $x_r[n]$ and $y_r[n]$ are the transmitted and received signal processes at the relay, respectively; $y_d[n]$ is the received signal process at the destination; and the noise processes $w_r[n]$ at the relay and $w_d[n]$ at the destination are independent zero-mean white Gaussian processes with variance σ^2 .

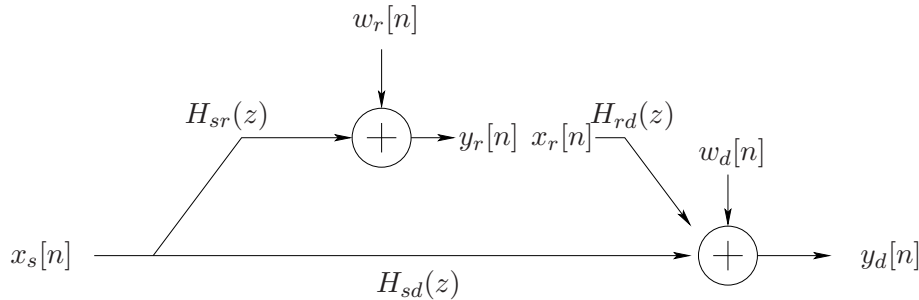


Fig. 1

SYSTEM MODEL

We consider the linear and causal processing at the relay. The general causal linear processing at the relay is given by

$$x_r[n] = \sum_{l \leq n} d_{nl} y_r[l], \quad (3)$$

for arbitrary linear combination coefficients d_{nl} , as considered in [3, 4]. However, such linear processing requires time-varying filtering at the relay, and is not readily realizable. Thus, in this paper, we restrict ourselves to the case of LTI causal filtering at the relay, as shown in Fig. 2. In this case, the relay output

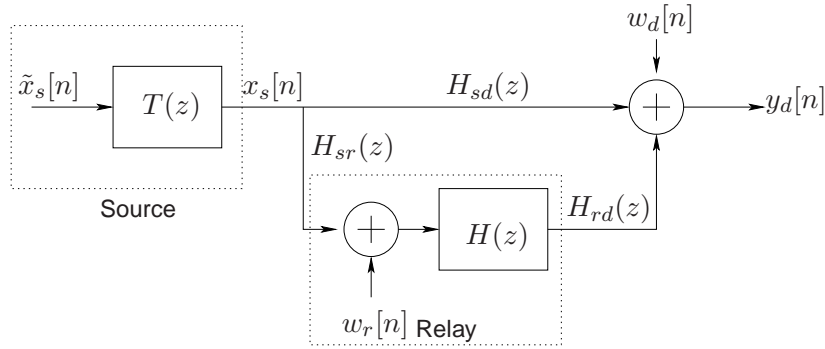


Fig. 2

SYSTEM MODEL WITH LINEAR TIME-INVARIANT FILTERS

is given by

$$x_r[n] = \sum_{l=0}^{\infty} h_l y_r[n-l], \quad (4)$$

where $[h_0, h_1, h_2, \dots]$ is the time-invariant impulse response of the relay filter and its z -transform is given by $H(z) = \sum_{l=0}^{\infty} h_l z^{-l}$. (In the case of strict causality, we have $h_0 = 0$.) The received signal (4) at the relay can be written in matrix form as (5), and the filtering matrix \mathbf{H}_n in (5) has a Toeplitz structure.

$$\begin{bmatrix} x_r[0] \\ x_r[1] \\ \vdots \\ x_r[n-1] \end{bmatrix} = \underbrace{\begin{bmatrix} h_0 & 0 & \cdots & \cdots & 0 \\ h_1 & h_0 & 0 & \cdots & 0 \\ h_2 & h_1 & h_0 & 0 & \vdots \\ \vdots & \ddots & \ddots & \ddots & 0 \\ h_{n-1} & \cdots & h_2 & h_1 & h_0 \end{bmatrix}}_{=:\mathbf{H}_n} \begin{bmatrix} y_r[0] \\ y_r[1] \\ \vdots \\ y_r[n-1] \end{bmatrix} + \begin{bmatrix} w_r[0] \\ w_r[1] \\ \vdots \\ w_r[n-1] \end{bmatrix}. \quad (5)$$

We assume the stability (i.e., $\sum_{l=0}^{\infty} |h_l| < \infty$) and *realizability*[†] for the relay filter. Since all processing from the source and to the destination is linear and time-invariant, the received signal at the destination in the z -domain is given by

$$Y_d(z) = (H_{sd}(z) + H_{rd}(z)H(z)H_{sr}(z))X_s(z) + H_{rd}(z)H(z)W_r(z) + W_d(z), \quad (6)$$

where $W_r(z)$ and $W_d(z)$ are the z -transforms of noise processes $w_r[n]$ and $w_d[n]$, respectively.

[†]It means that the LTI response $H(z)$ has a rational transfer function and it can readily be implemented by an autoregressive moving-average (ARMA) filter [17].

A. Background

In this subsection, we briefly summarize some relevant results including the eigen-structure of Toeplitz matrices and the spectral factorization for the development in later sections. For a zero-mean[‡] stationary random process $y[n]$, the covariance sequence and its z -spectrum are given by

$$r_y[k] = \mathbb{E}\{y[n]y^*[n-k]\} = r_y^*[-k] \quad \text{and} \quad S_y(z) := \sum_{k=-\infty}^{\infty} r_y[k]z^{-k} = \mathbb{E}\{Y(z)y[0]\}, \quad (7)$$

respectively, where $Y(z) = \sum_n y[n]z^{-n}$. The covariance matrix of a finite collection $\mathbf{y}_n := [y[0], y[1], \dots, y[n-1]]^T$ is given by

$$\Sigma_n^y := \mathbb{E}\{\mathbf{y}_n \mathbf{y}_n^H\} = \begin{bmatrix} r_y[0] & r_y[-1] & \cdots & r_y[-n+1] \\ r_y[1] & r_y[0] & & \vdots \\ \vdots & \vdots & \ddots & r_y[-1] \\ r_y[n-1] & r_y[n-2] & \cdots & r_y[0] \end{bmatrix}. \quad (8)$$

Theorem 1 (Asymptotic eigen-structure of Toeplitz covariance matrices [12], p. 135) Let $r_y[k]$ be an absolutely summable autocovariance sequence of a stationary process $y[n]$, let $S_y(e^{j\omega})$ be its power spectral density (PSD), i.e., $S_y(e^{j\omega}) = S_y(z)|_{z=e^{j\omega}}$, and let \mathbf{D}_n be the $n \times n$ matrix,

$$\mathbf{D}_n = \text{diag}(S_y(e^{j0}), S_y(e^{j\omega_1}), S_y(e^{-j\omega_1}), \dots, S_y(e^{j\omega_{(n-1)/2}}), S_y(e^{-j\omega_{(n-1)/2}})),$$

where $\omega_l = \frac{2\pi l}{n}$. Then, for the covariance matrix $\Sigma_n^y = [r_y[k-l]]_{k,l=1}^n$, the components of $\mathbf{X}^{(n)} := \mathbf{W}\Sigma_n^y\mathbf{W}^{-1} - \mathbf{D}_n$ converge to zero uniformly as $n \rightarrow \infty$ (i.e. $\sup_{1 \leq k, l \leq n} |\mathbf{X}^{(n)}(k, l)| \rightarrow 0$), where \mathbf{W} is the discrete Fourier transform (DFT) matrix.

For even n , we have a similar result with a slight modification. Theorem 1 simply states that the eigenvalues of the Toeplitz covariance matrix of a stationary process are the uniform samples of its spectrum. Using Theorem 1, the following can easily be shown.

Theorem 2 (Toeplitz distribution theorem [11], p. 65) Let $\{\lambda_i^{(n)}\}$ be the eigenvalues of the Toeplitz covariance matrix Σ_n^y of a stationary process $y[n]$. Then,

$$\lim_{n \rightarrow \infty} \frac{1}{n} \sum_{i=1}^n f(\lambda_i^{(n)}) = \frac{1}{2\pi} \int_{-\pi}^{\pi} f(S_y(e^{j\omega})) d\omega \quad (9)$$

for any continuous function $f(\cdot)$.

[‡] In the case of a known non-zero mean, the mean of the process can be subtracted and the result can still be applied.

In addition to the asymptotic eigen-structure of Toeplitz covariance matrices, we need some background in the spectral theory for stationary random processes, especially canonical spectral factorization.

Definition 1 (Canonical Spectral Factorization [18], p. 197) Let $S_y(z)$ be a rational z-spectrum of a finite power process and assume that $S_y(z)$ is strictly positive. Then, the canonical spectral factorization of $S_y(z)$ is given by

$$S_y(z) = L(z)\gamma_e L^\sharp(z), \quad (10)$$

where $L(z) = \sum_{i=0}^{\infty} l_i z^{-i}$ is a unique stable, causal, monic and minimum-phase (SCAMP) filter (i.e., the zeros and poles of $L(z)$ are strictly inside the unit circle and $L(\infty) = 1$ (or equivalently $l_0 = 1$)), and $\gamma_e > 0$. Here, $L^\sharp(z) := L^*(z^{-*})$ denotes the para-Hermitian conjugate.

III. THE RATE FORMULA IN FREQUENCY-DOMAIN FOR LTI RELAYS

First, note that the overall channel model (6) with LTI relay filtering is still a linear additive *stationary* Gaussian noise channel. Thus, for a given relay filter, the overall channel with the LTI relay filter reduces back to the classical ISI channel with stationary Gaussian noise[§]. In this case, stationary Gaussian signal processes with well-defined spectra are sufficient to achieve the capacity [13, pp. 407 - 430]. Hence, we assume that the source (or input) process $x_s[n]$ is a stationary Gaussian process. By concatenating symbols at the source up to time $n - 1$, we have

$$\mathbf{x}_n^s := [x_s[0], x_s[1], \dots, x_s[n-1]]^T \sim \mathcal{N}(\mathbf{0}, \mathbf{\Sigma}_n^{x_s}), \quad (11)$$

and vectors \mathbf{y}_n^r , \mathbf{x}_n^r and \mathbf{y}_n^d are constructed similarly for the relay and destination nodes. Then, the power constraints for the source and relay are respectively given by

$$(1/n)\text{tr}(\mathbf{\Sigma}_n^{x_s}) \leq P_s, \quad \text{and} \quad (12)$$

$$(1/n)\mathbb{E}\{\text{tr}(\mathbf{H}_n \mathbf{y}_r^n (\mathbf{H}_n \mathbf{y}_r^n)^H)\} = (1/n)\text{tr}(\mathbf{H}_n (\mathbf{H}_n^{sr} \mathbf{\Sigma}_n^{x_s} \mathbf{H}_n^{sr} + \sigma^2 \mathbf{I}) \mathbf{H}_n^H) \leq P_r, \quad (13)$$

where \mathbf{H}_n^{sr} is the filtering matrix for the S-R channel constructed based on $\{h_{sr}[l]\}$ similar to \mathbf{H}_n in (5). Thus, the maximum rate with LTI relaying for block size n is given by maximizing the mutual information between \mathbf{x}_n^s and \mathbf{y}_n^d over $\mathbf{\Sigma}_n^{x_s}$ and \mathbf{H}_n under power constraints (12) and (13), and the capacity with LTI relaying is given by its limit

$$C_{LTI} = \lim_{n \rightarrow \infty} \sup_{\mathbf{\Sigma}_n^{x_s}, \mathbf{H}_n} \frac{1}{n} I(\mathbf{x}_n^s; \mathbf{y}_n^d), \quad (14)$$

[§]However, the major difference between the two problems is that in the relay problem we even have to design the overall channel by properly choosing the relay filter and the power constraints at the source and relay are intertwined.

as $n \rightarrow \infty$ [4], where

$$\begin{aligned} I(\mathbf{x}_n^s; \mathbf{y}_n^d) &= H(\mathbf{y}_n^d) - H(\mathbf{y}_n^d | \mathbf{x}_n^s), \\ &= \log |\sigma^2 \mathbf{H}_n^{rd} \mathbf{H}_n \mathbf{H}_n^H (\mathbf{H}_n^{rd})^H + \sigma^2 \mathbf{I} + (\mathbf{H}_n^{sd} + \mathbf{H}_n^{rd} \mathbf{H}_n \mathbf{H}_n^{sr}) \Sigma_n^{x_s} (\mathbf{H}_n^{sd} + \mathbf{H}_n^{rd} \mathbf{H}_n \mathbf{H}_n^{sr})^H| \\ &\quad - \log |\sigma^2 \mathbf{H}_n^{rd} \mathbf{H}_n \mathbf{H}_n^H (\mathbf{H}_n^{rd})^H + \sigma^2 \mathbf{I}|. \end{aligned} \quad (15)$$

Here, \mathbf{H}_n^{sd} and \mathbf{H}_n^{rd} are the filtering matrices for the S-D and R-D channels, respectively. Note that (14) is still valid for general linear time-varying relay filtering with \mathbf{H}_n given by an arbitrary lower triangular matrix. As mentioned in [4], the computation of capacity and the design of capacity-achieving (or at least reasonable) $\Sigma_n^{x_s}$ and \mathbf{H}_n are difficult problems in the case of general linear causal relay filtering. In the time-varying case, if we increase n by one, at least $2n$ new variables $\{\Sigma_n^{x_s}(n, 1), \Sigma_n^{x_s}(n, 2), \dots, \Sigma_n^{x_s}(n, n), d_{n1}, d_{n2}, \dots, d_{nn}\}$ appear (see (3)), and thus the complexity of the problem increases with the order of $n!$ to make the problem difficult [3,4]. In the LTI case with a stationary source process, however, we have only two new variables $r_{x_s}[n-1]$ and h_{n-1} for the increase of the problem size from $n-1$ to n because of the Toeplitz structure of the covariance matrix in (8) and the filtering matrix in (5). Following the best input covariance matrix and relay filter for the problem size n is equivalent to designing the best infinitely long autocovariance sequence $\{r_{x_s}[k], k = 0, 1, \dots\}$ and infinitely long relay filter $\{h_l, l = 0, 1, \dots\}$ first and then increasing the problem size. Thus, in the LTI case, we have

$$C_{LTI} = \sup_{\{r_{x_s}[k]\}, H(z)} \lim_{n \rightarrow \infty} \frac{1}{n} \left[I(\mathbf{x}_n^s; \mathbf{y}_n^d) | \Sigma_n^{x_s}(\{\gamma_{x_s}[k]\}), \mathbf{H}_n(H(z)) \right], \quad (16)$$

where the respective dependence of $\Sigma_n^{x_s}$ and \mathbf{H}_n on $\{r_{x_s}[k]\}$ and $H(z)$ is explicitly shown. Here, taking the limit of n simplifies the problem significantly due to Theorem 2 since the eigenvalues are strictly positive due to the additive noise term and since $f(t) = \log(t)$ is a continuous function of t for $t > 0$. By Theorems 1 and 2 we have

$$C_{LTI} = \sup_{S_{x_s}(e^{j\omega}), H(z)} \frac{1}{2\pi} \int_{-\pi}^{\pi} \frac{1}{2} \log_2 \left(1 + \frac{|H_{sd}(e^{j\omega}) + H_{sr}(e^{j\omega})H(e^{j\omega})H_{rd}(e^{j\omega})|^2}{\sigma^2(|H_{rd}(e^{j\omega})H(e^{j\omega})|^2 + 1)} S_{x_s}(e^{j\omega}) \right) d\omega, \quad (17)$$

where the input spectrum $S_{x_s}(e^{j\omega}) = \sum_{k=-\infty}^{\infty} r_{x_s}[k] e^{-j\omega k}$, since the eigenvalues of a covariance matrix are the samples of its spectrum and the determinant of a covariance matrix is the product of its eigenvalues.

Here, we define the overall channel-to-noise power ratio (CNR) density as

$$\text{CNR}(e^{j\omega}) := \frac{|H_{sd}(e^{j\omega}) + H_{sr}(e^{j\omega})H(e^{j\omega})H_{rd}(e^{j\omega})|^2}{\sigma^2(|H_{rd}(e^{j\omega})H(e^{j\omega})|^2 + 1)} = \frac{N(e^{j\omega})}{D(e^{j\omega})}, \quad (18)$$

where $N(e^{j\omega})$ and $D(e^{j\omega})$ are the numerator and denominator of the CNR density, respectively. Note that the CNR density captures the overall channel response from source to destination. When the CNR density

is multiplied by the input signal PSD, the product becomes the overall SNR density at the destination. (This quantity will be used in later sections.) In addition to the rate formula (17) in the frequency domain, the power constraints can also be expressed in the frequency domain as $n \rightarrow \infty$. As $n \rightarrow \infty$, again by Theorems 1 and 2, the power constraints (12) and (13) are respectively given by

$$\frac{1}{2\pi} \int_{-\pi}^{\pi} S_{x_s}(e^{j\omega}) d\omega \leq P_s, \quad \text{and} \quad (19)$$

$$\frac{1}{2\pi} \int_{-\pi}^{\pi} |H(e^{j\omega})|^2 (|H_{sr}(e^{j\omega})|^2 S_{x_s}(e^{j\omega}) + \sigma^2) d\omega \leq P_r, \quad (20)$$

since the trace of a matrix is the sum of its eigenvalues. Thus, the LTI relay problem is summarized by (17), (19) and (20). Note that for a given relay filter $H(z)$ the problem without the power constraint (20) reduces to the well-known ISI channel problem and the solution of $S_{x_s}(e^{j\omega})$ is given by water-filling in the frequency domain [19]. However, the freedom to design $H(z)$ and the relay power constraint (20) make the problem far more difficult than the simple ISI channel problem. To construct a practical method to solve this problem, we further assume that the input spectrum $S_{x_s}(e^{j\omega})$ is also *realizable*. That is, its canonical spectral factorization is given by

$$S_{x_s}(z) = \alpha \tilde{T}(z) \tilde{T}^\#(z) = T(z) T^\#(z), \quad (T(z) = \sqrt{\alpha} \tilde{T}(z)), \quad (21)$$

where the SCAMP filter $\tilde{T}(z)$ has a rational transfer function and, thus, $S_{x_s}(z)$ is a rational spectrum. In this case, the source process $x_s[n]$ can be modelled as the output of the stable and causal ARMA filter $T(z)$ driven by a white Gaussian process $\tilde{x}_s[n]$ with unit variance, as seen in Fig. 2. Thus, the rate maximization problem under *LTI relaying with realizable input spectra* now reduces to a *joint design problem of LTI source and relay filters*. Obtaining the capacity in a closed form still seems to be a difficult problem even in the LTI relay case. However, we propose a very effective and practical solution to this joint filter design problem in Section V. Before we tackle this problem, we investigate the problem in the case that all S-D, S-R and R-D channels have flat frequency responses in the next section.

IV. EXAMINATION OF LTI RELAYING IN FLAT-FADING CHANNELS

In the case of flat fading, we have the system model (6) in which each of S-R, R-D and S-D channels has only one tap, i.e., $H_{sd}(z) = 1$, $H_{sr}(z) = a$ and $H_{rd}(z) = b$, as considered in [3, 4]. Then, the received signal model in the z -domain is given by

$$Y_d(z) = (1 + abH(z))X_s(z) + bH(z)W_r(z) + W_d(z). \quad (22)$$

A. The One-Tap Relay Filter Case

First, consider the well-known AF relaying. In this case, we have

$$x_r[n] = dy_r[n],$$

where $\mathbb{E}\{x_s^2\} = P_s$ and $0 \leq d \leq \sqrt{\frac{P_r}{a^2 P_s + \sigma^2}} =: d_{max}$ to satisfy the power constraints, and the received signal model is given by

$$y_d[n] = (1 + abd)x_s[n] + bdw_r[n] + w_d[n]. \quad (23)$$

Due to the simple data model (23), the achievable rate in this case is known and given by

$$R_{AF} = \max_{0 \leq d \leq d_{max}} \frac{1}{2} \log \left(1 + \frac{(1 + abd)^2}{b^2 d^2 + 1} \cdot \frac{P_s}{\sigma^2} \right), \quad (24)$$

and the optimal value of d is explicitly given by

$$d^* = \min \left\{ \frac{a}{b}, \sqrt{\frac{P_r}{a^2 P_s + \sigma^2}} \right\}. \quad (25)$$

Now consider the one-tap LTI relay filter with an arbitrary delay:

$$H(z) = dz^{-\Delta} \quad (26)$$

for some integer $\Delta \geq 0$ [¶], where the relay gain d can be optimized under the power constraints. Note in the system model (22) that the relay filter affects both the channel gain and noise spectrum. However, in the one-tap relay filter case, the problem is simplified because the overall noise spectrum is white. In this case, the overall channel gain is given by $1 + abH(z) = 1 + abd z^{-\Delta}$ and the overall noise spectrum is given by

$$\begin{aligned} b^2 H(z) H^\#(z) \sigma^2 + \sigma^2 &= b^2 \sigma^2 (dz^{-\Delta})(dz^{-\Delta})^\# + \sigma^2, \\ &= (b^2 d^2 + 1) \sigma^2, \end{aligned}$$

since $(z^{-\Delta})^\# = z^\Delta$. Note that the overall noise process in this case is white and equivalent to that in the AF data model (23); both have the same variance $(b^2 d^2 + 1) \sigma^2$. Thus, the spectrum of $Y_d(z)$ is given by

$$S_{y_d}(e^{j\omega}) = |1 + abH(e^{j\omega})|^2 S_{x_s}(e^{j\omega}) + (b^2 d^2 + 1) \sigma^2, \quad (27)$$

and the channel frequency response is explicitly given by a raised-cosine function:

$$\begin{aligned} |1 + abH(e^{j\omega})|^2 &= (1 + abde^{-j\omega\Delta})(1 + abde^{j\omega\Delta}), \\ &= 1 + 2abd \cos(\omega\Delta) + a^2 b^2 d^2 \geq 0. \end{aligned} \quad (28)$$

[¶]Note that strict causality implies $\Delta > 0$.

Since $|H(e^{j\omega})|^2 = d^2$ for $H(z) = dz^{-\Delta}$, from (19) and (20) the power constraints are given by

$$\frac{1}{2\pi} \int_{-\pi}^{\pi} S_{x_s}(e^{j\omega}) d\omega \leq P_s, \quad \text{and} \quad (29)$$

$$\frac{d^2}{2\pi} \int_{-\pi}^{\pi} (a^2 S_{x_s}(e^{j\omega}) + \sigma^2) d\omega = d^2 \left(a^2 \frac{1}{2\pi} \int_{-\pi}^{\pi} S_{x_s}(e^{j\omega}) d\omega + \sigma^2 \right) \leq P_r, \quad (30)$$

which are the same as those of the AF scheme with $\Delta = 0$.

The problem with the given relay filter $H(z) = dz^{-\Delta}$ reduces to the simple ISI channel problem, and the optimal input spectrum $S_{x_s}^*(e^{j\omega})$ is obtained by water-filling under the two simple power constraints (29) and (30). In the following theorem, we establish the optimality of the AF scheme within the class of all one-tap relay filters.

Theorem 3: Among all one-tap linear relay filters, i.e., $H(z) = dz^{-\Delta}$ with $\Delta \in \mathbb{I}$, the AF scheme with $\Delta = 0$ maximizes the achievable rate.

Proof: For a given $\Delta \neq 0$, let

$$(S_{x_s}^*(e^{j\omega}), d^*) = \arg \max_{S_{x_s}(e^{j\omega}), d} \frac{1}{2\pi} \int_{-\pi}^{\pi} \frac{1}{2} \log \left(1 + \frac{|1 + abde^{-j\omega\Delta}|^2}{(b^2 d^2 + 1)\sigma^2} S_{x_s}(e^{j\omega}) \right) d\omega. \quad (31)$$

Then,

$$\begin{aligned} & \frac{1}{2\pi} \int_{-\pi}^{\pi} \frac{1}{2} \log \left(1 + \frac{|1 + abd^* e^{-j\omega\Delta}|^2}{(b^2 d^{*2} + 1)\sigma^2} S_{x_s}^*(e^{j\omega}) \right) d\omega \\ & \leq \frac{1}{2\pi} \int_{-\pi}^{\pi} \frac{1}{2} \log \left(1 + \frac{(1 + abd^*)^2}{(b^2 d^{*2} + 1)\sigma^2} S_{x_s}^*(e^{j\omega}) \right) d\omega, \end{aligned} \quad (32)$$

$$\leq \sup_{S_{x_s}(e^{j\omega}), d} \frac{1}{2\pi} \int_{-\pi}^{\pi} \frac{1}{2} \log \left(1 + \frac{(1 + abd)^2}{(b^2 d^2 + 1)\sigma^2} S_{x_s}(e^{j\omega}) \right) d\omega, \quad (33)$$

$$\leq \sup_{S_{x_s}(e^{j\omega}), d} \frac{1}{2} \log \left(1 + \frac{(1 + abd)^2}{(b^2 d^2 + 1)\sigma^2} \frac{1}{2\pi} \int_{-\pi}^{\pi} S_{x_s}(e^{j\omega}) d\omega \right), \quad (34)$$

$$= R_{AF}. \quad (35)$$

Here, (32) is obtained because $|1 + abd^* e^{-j\omega\Delta}|^2 \leq (1 + abd^*)^2$. (33) is obtained because the feasible set $(S_{x_s}(e^{j\omega}), d)$ satisfying the power constraint for $\Delta \neq 0$ is the same as that for $\Delta = 0$ when $H(z) = dz^{-\Delta}$. (See (29) and (30).) (34) is obtained by Jensen's inequality. Finally, (35) is obtained by the definition of R_{AF} in (24). \blacksquare

Theorem 3 states that the AF scheme with $\Delta = 0$ performs best within the class of one-tap relay filters with arbitrary delays. This is because the AF scheme achieves coherent signal combining between the two signal paths S-D and S-R-D. Instead of using the optimal water-filling source filter, we can also consider

a simple channel-equalizing source filter. However, the performance in this case is bad, as shown in the following theorem.

Theorem 4: The achievable rate by an equalizing source filter for the one-tap relay filter $H(z) = dz^{-\Delta}$ is given by

$$R_{1\text{-tap, EQ}} = \sup_{0 \leq d < \min\{d_{max}, \frac{1}{ab}\}} \frac{1}{2} \log \left(1 + \frac{1 - (abd)^2}{b^2 d^2 + 1} \cdot \frac{P_s}{\sigma^2} \right) \quad (36)$$

regardless of the value of $\Delta > 0$. Further, the supremum is given by $R_{1\text{-tap, EQ}} = \frac{1}{2} \log \left(1 + \frac{P_s}{\sigma^2} \right)$ achieved when $d = 0$.

Proof: We have $X_s(z) = \sqrt{\alpha} \tilde{T}(z) \tilde{X}_s(z)$, where $\tilde{X}_s(z)$ is the z -transform of the white Gaussian process $\tilde{x}_s[n]$ with unit variance, and the equalizing source filter is given by

$$\tilde{T}(z) = \frac{1}{1 + abH(z)} = \frac{1}{1 + abd z^{-\Delta}} = 1 - abd z^{-\Delta} + (abd)^2 z^{-2\Delta} - (abd)^3 z^{-3\Delta} + \dots$$

When $0 \leq d < \frac{1}{ab}$, the overall channel response $1 + abH(z)$ is SCAMP and, thus, the channel-equalizing source filter $\tilde{T}(z)$ is also SCAMP. By the power constraint at the source, we have

$$\frac{1}{2\pi} \int_{-\pi}^{\pi} S_{x_s}(e^{j\omega}) d\omega = \frac{\alpha}{2\pi} \int_{-\pi}^{\pi} \frac{1}{1 + 2abd \cos(\omega\Delta) + (abd)^2} d\omega = P_s \quad (37)$$

because $S_{x_s}(z) = \alpha \tilde{T}(z) \tilde{T}^\#(z)$. Since $\int_{-\pi}^{\pi} \frac{1}{1 + 2abd \cos(\omega\Delta) + (abd)^2} d\omega = \frac{2\pi}{1 - (abd)^2}$ for every integer $\Delta > 0$, $\alpha = (1 - (abd)^2) P_s$ regardless of the value of $\Delta > 0$. With the channel-equalizing source filter $T(z) = \sqrt{\alpha} \tilde{T}(z)$, the data model is given by $y_d[n] = \sqrt{\alpha} \tilde{x}_s[n] + w_{eff}[n]$, where $\tilde{x}_s[n] \sim \mathcal{N}(0, 1)$ and $w_{eff}[n] \sim \mathcal{N}(0, (b^2 d^2 + 1)\sigma^2)$, and the corresponding achievable rate is given by (36). Now consider $\text{CNR}(d) = \frac{1 - (abd)^2}{b^2 d^2 + 1} \frac{1}{\sigma^2}$ in (36). Its derivative with respect to (w.r.t.) d is given by $\text{CNR}'(d) = [-2a^2 b^2 d (b^2 d^2 + 1) - (1 - a^2 b^2 d^2) 2b^2 d] / [(b^2 d^2 + 1)^2 \sigma^2] \leq 0$ for all $d \geq 0$. Thus, the rate is maximized when $d = 0$. ■

Theorem 4 states that it is optimal to turn off the (one-tap) relay filter when the channel-equalizing filter is to be used at the source. Thus, using the channel-equalizing source filter is not a proper choice for relay networks.

Fig. 3 shows the achievable rates of several relaying schemes. For Fig. 3 (a) and (b), which show the same curves with two different x-axis ranges, we set $a = 1$ and $b = 2$, as in [4]. It is seen that simple linear strictly causal schemes (one based on the filtering matrix $\begin{bmatrix} 0 & 0 \\ d & 0 \end{bmatrix}$ in [4] and the other based on one-tap filtering $H(z) = dz^{-1}$) can outperform the CF scheme in the low SNR region, as already known from [4]. In this case of $a = 1$ and $b = 2$, the AF scheme achieves the cut-set upperbound for $P_s = P_r \geq 1/3$ [6, Proposition 9]. It is interesting to observe that the simple linear scheme in [4] with $n = 2$ performs

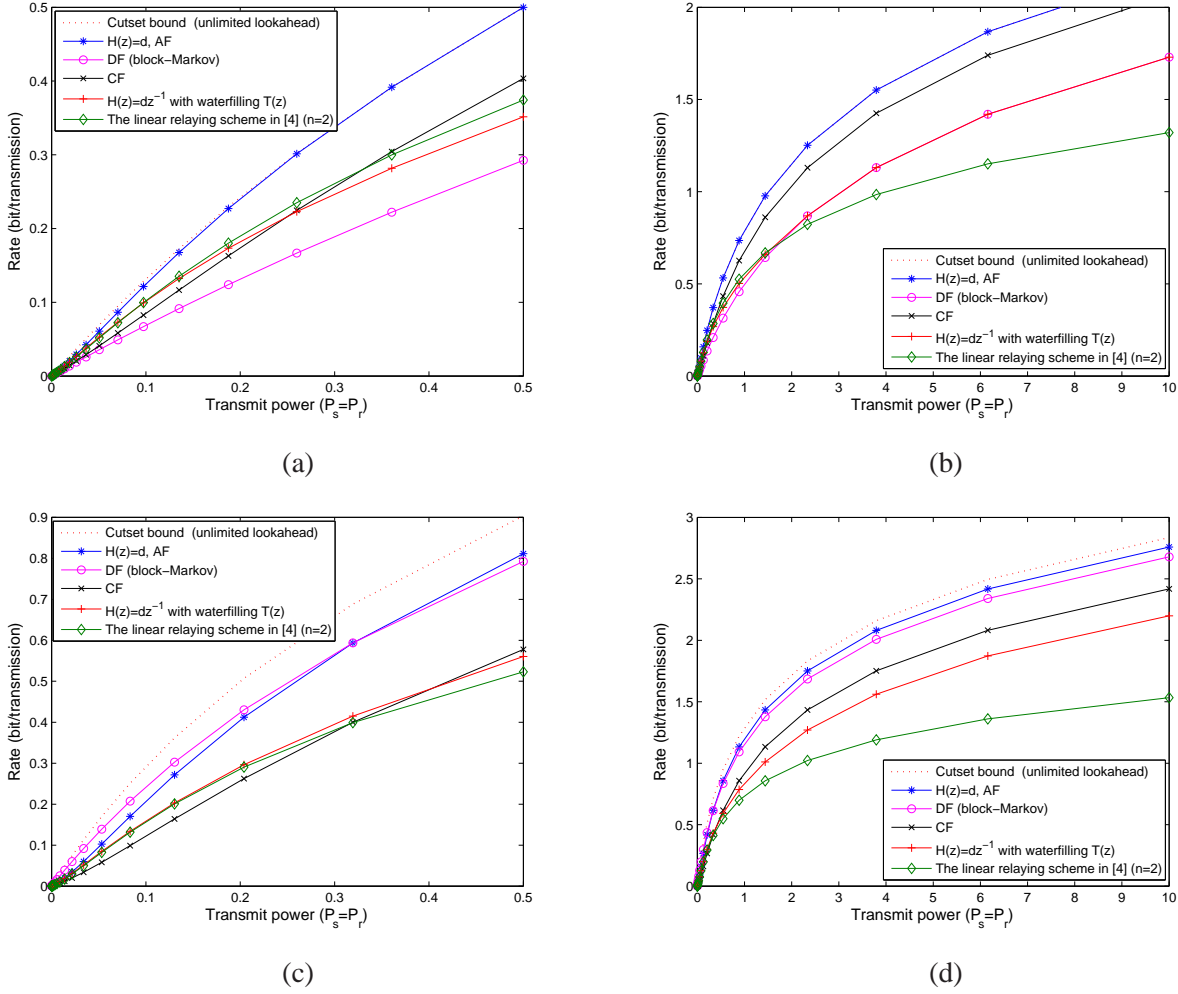


Fig. 3

ACHIEVABLE RATES OF SEVERAL SCHEMES IN FLAT-FADING CHANNELS ($P_s = P_r, \sigma^2 = 1$) - (A) AND (B):

$$a = 1, b = 2, \text{ AND (C) AND (D): } a = 2, b = 2$$

better than $H(z) = dz^{-1}$ filtering in some low SNR values, although the latter outperforms the former eventually at high SNR. Fig. 3 (c) and (d), again showing the same curves in two different x-axis ranges, show the achievable rates when $a = b = 2$. In this case, it is seen that there is a gap between the cut-set bound and the AF scheme. In all the cases, it is seen that the two strictly causal linear schemes (one based on two-symbol concatenation in [4] and the other based on one-tap LTI filtering $H(z) = dz^{-1}$) do not outperform the AF scheme, as expected by Theorem 3.

B. The Multiple-Tap Relay Filter Case: Insights from Ideal Low-Pass Filtering Relays

In Section IV-A, it is shown that one-tap relay filters do not outperform the AF scheme in flat-fading channels. This is because any one-tap relay filter with a causal or non-causal non-zero delay cannot change the noise spectrum, but destroys the coherent combining that is available in the AF scheme. However, this is not the case when the relay filter has multiple taps. In this case, the overall noise spectrum as well as the channel gain spectrum in (22) can be shaped by the relay filter, and the LTI relaying scheme with multiple taps can outperform the AF scheme in flat-fading channels. However, the performance analysis in this case is far more difficult than that in the one-tap relay case, especially when the causality constraint is imposed on the relay filter. To circumvent this difficulty, in this subsection we relax the causality constraint on $H(z)$ and consider the tractable ideal low-pass^{||} relay filtering to gain insights into the interaction between the source and relay filters and to assess the rate gain that can be obtained by multiple-tap relay filtering. The frequency response of the ideal low-pass relay filter is given by

$$H(e^{j\omega}) = \begin{cases} \delta, & |\omega| < \omega_c, \\ 0, & \omega_c < |\omega| < \pi, \end{cases} \quad (38)$$

where δ is the passband gain and ω_c is the cutoff frequency. For a given ω_c , the optimization problem (17,19,20) with the ideal low-pass relay filter is expressed as

$$\max_{\delta, S_{x_s}(e^{j\omega})} \left[\frac{1}{\pi} \int_0^{\omega_c} \frac{1}{2} \log_2 \left(1 + \frac{(1+abd)^2}{(b^2\delta^2+1)\sigma^2} S_{x_s}(e^{j\omega}) \right) d\omega + \frac{1}{\pi} \int_{\omega_c}^{\pi} \frac{1}{2} \log_2 \left(1 + \frac{1}{\sigma^2} S_{x_s}(e^{j\omega}) \right) d\omega \right] \quad (39)$$

subject to

$$\frac{1}{\pi} \int_0^{\pi} S_{x_s}(e^{j\omega}) d\omega - P_s \leq 0 \quad (40)$$

$$\frac{1}{\pi} \int_0^{\omega_c} \delta^2 (a^2 S_{x_s}(e^{j\omega}) + \sigma^2) d\omega - P_r \leq 0 \quad (41)$$

$$S_{x_s}(e^{j\omega}) \geq 0, \quad \forall \omega \in [0, \pi], \quad (42)$$

where the even symmetry of spectra is used. Note that the problem is not jointly convex w.r.t. δ and $S_{x_s}(e^{j\omega})$ for a given ω_c . However, we can still apply the Karush-Kuhn-Tucker (KKT) conditions to this problem to obtain the necessary conditions for optimality [20]. The Lagrangian of this problem is given

^{||}Different types of ideal filters, i.e., high-pass, band-pass, band-stop filters, yield essentially the same result as the ideal low-pass filters when the bandwidth of passband is the same.

by

$$\mathcal{L} = -\frac{1}{\pi} \int_0^{\omega_c} \frac{1}{2} \log_2 \left(1 + \frac{(1+ab\delta)^2}{(b^2\delta^2+1)\sigma^2} S_{x_s}(e^{j\omega}) \right) d\omega - \frac{1}{\pi} \int_{\omega_c}^{\pi} \frac{1}{2} \log_2 \left(1 + \frac{1}{\sigma^2} S_{x_s}(e^{j\omega}) \right) d\omega \quad (43)$$

$$+ \lambda \left(\frac{1}{\pi} \int_0^{\pi} S_{x_s}(e^{j\omega}) d\omega - P_s \right) \quad (44)$$

$$+ \nu \left(\frac{1}{\pi} \int_0^{\omega_c} \delta^2 (a^2 S_{x_s}(e^{j\omega}) + \sigma^2) d\omega - P_r \right), \quad (45)$$

where λ and ν are non-negative dual variables. Due to the complementary slackness, either $\lambda = 0$ or the source uses full power, i.e., $\frac{1}{\pi} \int_0^{\pi} S_{x_s}(e^{j\omega}) d\omega = P_s$; and either $\nu = 0$ or the relay uses full power. Suppose that the source does not use full power. Then, the source can increase the PSD over the frequency band $[\omega_c, \pi]$ without changing the PSD over $[0, \omega_c]$. Then, the power constraint (41) at the relay is not affected and the rate in (39) increases. Thus, the source should use full power to yield maximum rate, and we have $\lambda > 0$ due to the complementary slackness. However, the relay may or may not use full power depending on the channel condition. The source PSD solution to the KKT conditions is given by a modified water-filling method:

$$S_{x_s}(e^{j\omega}) = \begin{cases} \left(\frac{1}{(2 \ln 2)(\lambda + \nu a^2 \delta^2)} - \frac{(b^2 \delta^2 + 1)\sigma^2}{(1 + ab\delta)^2} \right)^+, & |\omega| < \omega_c, \\ \left(\frac{1}{(2 \ln 2)\lambda} - \sigma^2 \right)^+, & \omega_c \leq |\omega| \leq \pi, \end{cases} \quad (46)$$

where $\gamma^+ := \max\{0, \gamma\}$. The optimal source PSD is given by the difference between the ‘water level’ and the overall effective ‘noise level’. The water level is a function of two dual variables λ and ν , and we may have two water levels if $\nu > 0$, i.e., the relay also uses full power. The effective noise level η is defined as the inverse of the overall CNR density, and it is given by $\eta_{pass} = \frac{b^2 \delta^2 + 1}{(1 + ab\delta)^2} \sigma^2$ and $\eta_{stop} = \sigma^2$ for $[0, \omega_c]$ and $[\omega_c, \pi]$, respectively. From here on, we will consider only the case $\eta_{pass} < \sigma^2$. (Otherwise, it is better not to use the relay ($\delta = 0$) since σ^2 over $[0, \pi]$ is the noise level without the relay.) To obtain optimal δ , we need to consider both (39) and (41). By differentiating $\eta_{pass}(\delta) = \frac{(b^2 \delta^2 + 1)\sigma^2}{(1 + ab\delta)^2}$ w.r.t. δ and setting the derivative to zero, we obtain $\delta = \frac{a}{b}$ for the minimum noise level $\eta_{pass}^* = (1 + a^2)\sigma^2 / (1 + a^2)^2$. However, we have the relay power constraint (41), yielding $\delta \leq \sqrt{P_r / (\frac{1}{\pi} \int_0^{\omega_c} a^2 S_{x_s}(e^{j\omega}) d\omega + \frac{\omega_c}{\pi} \sigma^2)} = \sqrt{P_r / (a^2 P_{pass} + (\omega_c / \pi) \sigma^2)}$, where P_{pass} is the portion of the source power allocated to the relay’s passband $[0, \omega_c]$ and $P_{stop} := P_s - P_{pass}$. Thus, the optimal δ^* is given by

$$\delta^* = \min \left\{ \frac{a}{b}, \sqrt{\frac{P_r}{a^2 P_{pass} + \frac{\omega_c}{\pi} \sigma^2}} \right\}, \quad (47)$$

since $\eta_{pass}(\delta)$ is monotonically increasing as δ decreases from a/b to zero. With the optimal δ^* , the multiple-tap relay filter generates a well in the noise level, as shown in Fig. 4. The effective noise level

$\eta_{pass}(\delta)$ of this well is equal to or lower than that of the AF scheme because the effective noise level for the AF scheme is $\eta_{AF}(d) = \frac{(b^2d^2+1)\sigma^2}{(1+abd)^2}$ for $-\pi \leq \omega \leq \pi$ (see (24)) and because for the same source power P_s and relay power P_r the upperbound for δ in (47) is larger than that for d in (25). (Note that $P_{pass} \leq P_s$ and $\omega_c \leq \pi$.) Thus, when P_r is small or $b \ll a$ such that (s.t.) $d^* < a/b$ (consequently, $\eta_{pass}(\delta) < \eta_{AF}(d)$), and P_s is also small enough to be confined within the passband well, the ideal low-pass filtering outperforms the AF scheme. (The amount of gain will be evaluated numerically shortly.)

The structure of solution $S_{x_s}(e^{j\omega})$ to the KKT conditions can be classified into four types depending on whether the source power is allocated to the relay's stopband $[\omega_c, \pi]$ or not, and whether the relay uses full power or not (equivalently, $\delta^* \neq a/b$ or not). Fig. 4 shows the solution types. A solution of Type 1

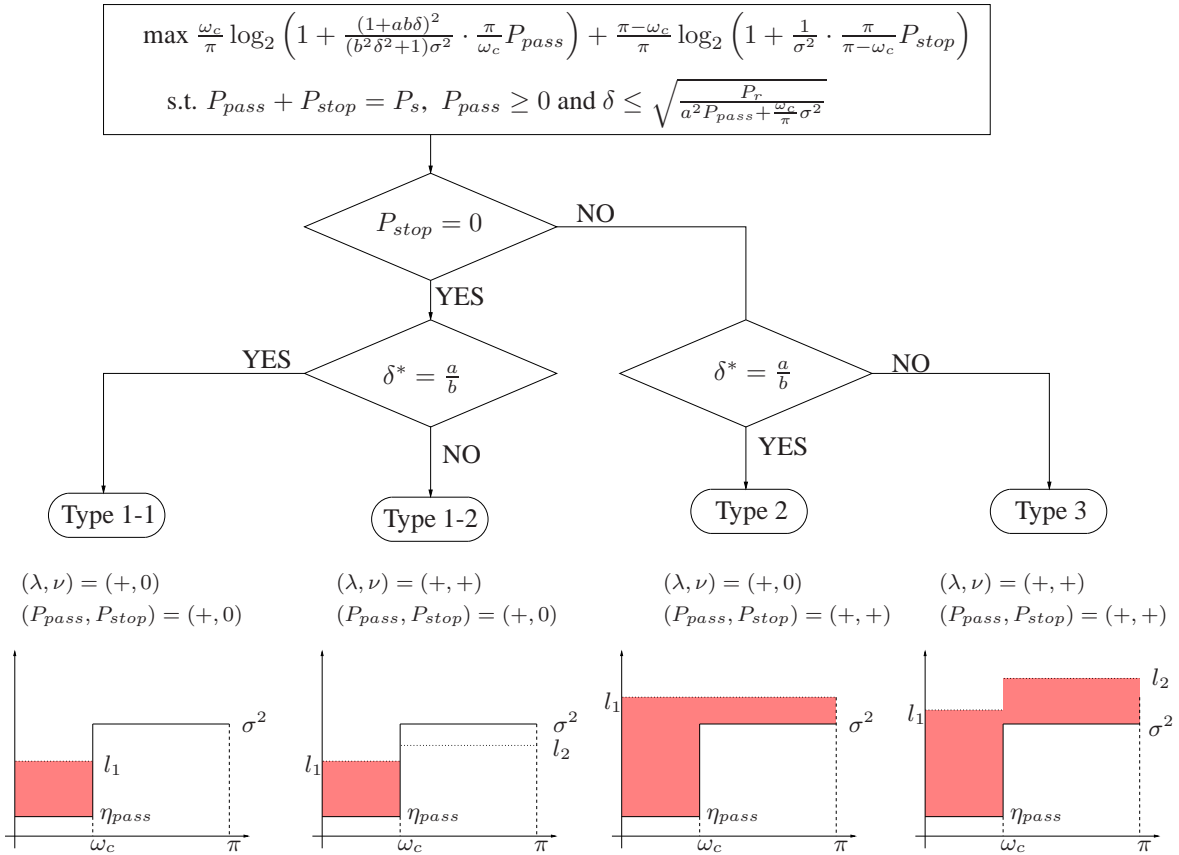


Fig. 4

DIFFERENT TYPES OF THE SOLUTION TO THE KKT CONDITIONS ($l_1 = \frac{1}{(2 \ln 2)(\lambda + \nu a^2 \delta^2)}$ AND $l_2 = \frac{1}{(2 \ln 2)\lambda}$)

occurs when all source power is allocated to the passband of the relay filter. We can further distinguish Type 1 depending on the power use of the relay. When the relay uses full power, both Lagrange dual variables λ and ν are positive, and there exist two water levels, although no water or power is allocated

in the stop band, i.e., $l_2 \leq \sigma^2$ (Type 1-2). Otherwise, we have Type 1-1 in which only λ is non-zero. A solution of Type 2 occurs when the relay does not use full power and the source power is allocated over the entire band; there is one water level common to both the passband and stopband. A Type 3 solution occurs when the relay uses full power and the source power is distributed over the entire band; both Lagrange dual variables are positive and the water levels at the passband and stopband are different. Different types of solutions occur for different combinations of parameters, P_s, P_r, σ^2, a, b , and ω_c .

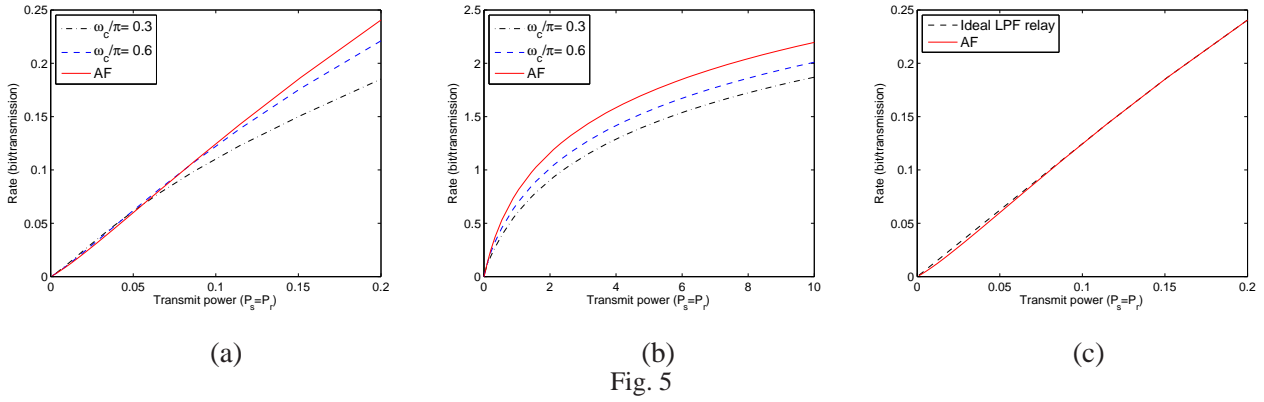


Fig. 5

RATE PERFORMANCE: IDEAL LOW-PASS RELAY FILTERING VERSUS AF ($P_s = P_r, \sigma^2 = 1, a = 1$ AND $b = 2$):

(A) FIXED ω_c (AT LOW P_s), (B) FIXED ω_c , AND (C) OPTIMIZED ω_c

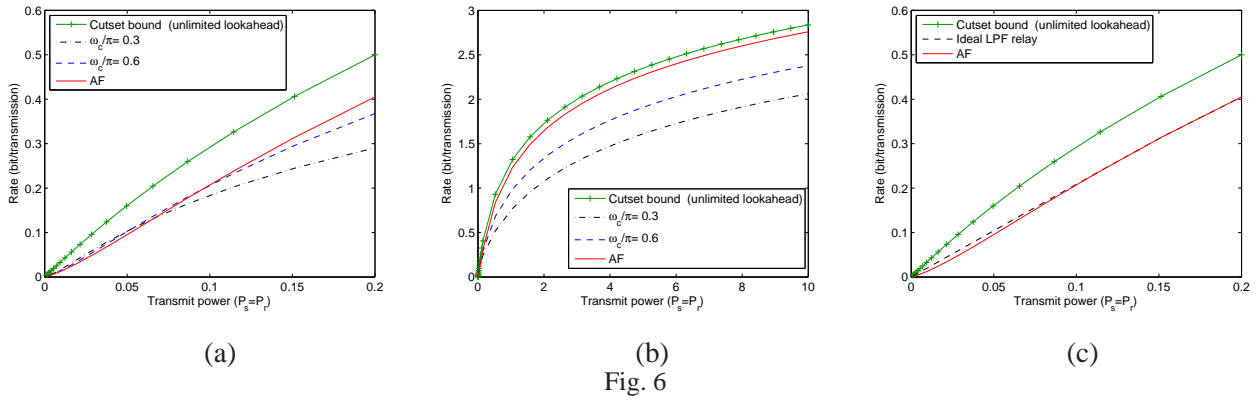


Fig. 6

RATE PERFORMANCE: IDEAL LOW-PASS RELAY FILTERING VERSUS AF ($P_s = P_r, \sigma^2 = 1, a = 2$ AND $b = 2$):

(A) FIXED ω_c (AT LOW P_s), (B) FIXED ω_c , AND (C) OPTIMIZED ω_c

To evaluate the performance of the ideal low-pass filtering at the relay, the optimization problem (39 - 42) was solved numerically using a commercial tool with δ and P_{pass} as variables for given P_s, P_r, σ^2, a, b and ω_c . First, we fixed $a = 1, b = 2$ and $\sigma^2 = 1$ (the same as for Fig. 3 (a) and (b)), and swept

$P_s = P_r$ for each $\omega_c \in \{0.3\pi, 0.6\pi\}$, and compared the performance of the ideal low-pass filtering with that of the AF scheme. The performance is shown in Fig. 5 (a) and (b). (The same rate curves are plotted with two different x-axis ranges.) It is seen in Fig. 5 (a) that indeed there is a gain over the AF scheme at the very low source power values. This is because the low-pass relay filter intentionally generates a well in the noise level in the passband and because all source power is allocated into this well at the very low source power values, as explained already. In this way, the signal is transmitted through a narrowband channel that has a lower noise level than that of the AF scheme. As P_s increases, however, the source power spills over the relay's stopband. At high SNR, the effect of the intentional noise level shaping is negligible (the effect of noise itself becomes negligible), and the uniform source power distribution over the entire frequency band is optimal at high SNR. Consequently, filtering out the signal existing at the stopband $[\omega_c, \pi]$ at the relay is detrimental to the performance at high SNR, as shown in Fig. 5 (a) and (b). So, we optimized the cut-off frequency ω_c together with δ and P_{pass} , and the result is shown in Fig. 5 (c). It is seen that the optimized solution shows the performance gain over the AF scheme at low SNR and eventually converges to the AF scheme as P_s increases. In this case of $a = 1$ and $b = 2$, the performance gain of the LPF relay over the AF scheme is not significant since the AF scheme performs well already, as shown in Fig. 3 (a) and (b) [6, Proposition 9]. Thus, we tried another case of $a = b = 2$ and $\sigma^2 = 1$ in which the AF scheme has a noticeable loss from the cut-set bound, as shown in Fig. 3 (c) and (d). Fig. 6 shows the achievable rate in this case. The figure shows similar behavior to the case of $a = 1$ and $b = 2$. One important fact here is that the performance gain of the ideal low-pass (multiple-tap) relay filtering (even breaking the causality constraint) over the AF scheme is not so significant in both of the cases. Thus, it seems that, practically, there is no need for complicated linear (time-invariant) filtering at the relay beyond the AF scheme in flat-fading channels. However, the insignificant gain is only for flat-fading channels, and this is not the case in realistic ISI channels. In the next section, we will tackle the LTI relay problem (17, 19, 20, 21) in ISI channels, propose a practical method to solve this problem, and show that the LTI relay filtering yields a noticeable gain over the AF scheme in ISI channels.

V. JOINT SOURCE AND RELAY FILTER DESIGN IN ISI CHANNELS

The LTI relay problem (17, 19, 20, 21) in ISI channels is basically a constrained optimization problem. Our approach to this problem is based on a powerful tool of the *projected subgradient method* developed by Polyak [14] and Yamada et al. [15, 16]. In the next subsection, we will briefly introduce their results that are relevant to our problem, and then move on to the original LTI relay problem.

A. Background: The Adaptive Projected Subgradient Method (APSM) [15, 16]

The projected subgradient method was initially proposed by Polyak [14] to solve cost minimization problems over convex constraint sets. Recently, Yamada et al. fully generalized the method even to adaptive situations with time-varying cost functions, and proved strong convergence of the method [15, 16].

Definition 2 (Subdifferential) Let $\phi : \mathcal{H} \rightarrow \mathbb{R}$ be a continuous convex function from a Hilbert space \mathcal{H} to the set \mathbb{R} of real numbers. Then, the *subdifferential* of ϕ at \mathbf{u} is defined as the set of all the subgradients of ϕ at \mathbf{u} :

$$\partial\phi(\mathbf{u}) := \{\mathbf{g} \in \mathcal{H} \mid \langle \mathbf{v} - \mathbf{u}, \mathbf{g} \rangle + \phi(\mathbf{u}) \leq \phi(\mathbf{v}), \forall \mathbf{v} \in \mathcal{H}\}, \quad (48)$$

where $\langle \cdot, \cdot \rangle$ is the inner product between two vectors.

Here, $\langle \mathbf{v} - \mathbf{u}, \mathbf{g} \rangle + \phi(\mathbf{u}) = r$ is a hyperplane with coordinates (\mathbf{v}, r) passing $(\mathbf{u}, \phi(\mathbf{u}))$ in the space $\mathcal{H} \times \mathbb{R}$. Thus, (48) implies that the hyperplane $\langle \mathbf{v} - \mathbf{u}, \mathbf{g} \rangle + \phi(\mathbf{u}) = r$ is below the cost surface $\phi(\mathbf{v}) = r$. It is known that $\partial\phi(\mathbf{u})$ is nonempty, and by definition we have $\mathbf{0} \in \partial\phi(\mathbf{u}) \Leftrightarrow \phi(\mathbf{u}) = \min_{\mathbf{v} \in \mathcal{H}} \phi(\mathbf{v})$. In the differentiable case, the gradient is a unique subgradient.

Definition 3 (Metric projection) The metric projection $P_K(\mathbf{u})$ of a point \mathbf{u} onto a closed convex set K is the closest point of \mathbf{u} in K , i.e., $\|P_K(\mathbf{u}) - \mathbf{u}\| \leq \|\mathbf{v} - \mathbf{u}\|, \forall \mathbf{v} \in K$.

Definition 4 (Subgradient projection) Suppose that a continuous convex function $\phi : \mathcal{H} \rightarrow \mathbb{R}$ satisfies $\text{lev}_{\leq 0}\phi := \{\mathbf{v} \in \mathcal{H} \mid \phi(\mathbf{v}) \leq 0\} \neq \emptyset$, i.e., the zero-level set is not empty. Let $\phi' : \mathcal{H} \rightarrow \mathcal{H}$ be a selection of the subdifferential $\partial\phi$, i.e., $\phi'(\mathbf{u}) \in \partial\phi(\mathbf{u}), \forall \mathbf{u} \in \mathcal{H}$. Then, a mapping $T_{sp(\phi)} : \mathcal{H} \rightarrow \mathcal{H}$ defined by

$$T_{sp(\phi)} : \mathbf{u} \mapsto \begin{cases} \mathbf{u} - \frac{\phi(\mathbf{u})}{\|\phi'(\mathbf{u})\|^2} \phi'(\mathbf{u}), & \text{if } \phi(\mathbf{u}) > 0 \\ \mathbf{u}, & \text{if } \phi(\mathbf{u}) \leq 0, \end{cases} \quad (49)$$

is called a *subgradient projection relative to ϕ* .

Here, the normalization of the subgradient by factor $\frac{\phi(\mathbf{u})}{\|\phi'(\mathbf{u})\|^2}$ is crucial to determining the step size parameter. Basically, the subgradient projection moves the current point \mathbf{u} to its metric projection onto the intersection of two hyperplanes $r = 0$ and $\langle \mathbf{v} - \mathbf{u}, \mathbf{g} \rangle + \phi(\mathbf{u}) = 0$ in the space of $\mathcal{H} \times \mathbb{R}$ with coordinates (\mathbf{v}, r) . (See [21, Fig.16].) It is known that the subgradient projection always moves the original point closer to every point in the zero-level set, which is known as the Fejér monotone property with respect to the zero-level set [16, 22]. It is also known that the subgradient projection belongs to the class of firmly quasi-nonexpansive mappings [16, 22]. Now, we state the adaptive projected subgradient theorem by Slavakis, Yamada and Ogura.

Theorem 5 (APSM, [15, 16]) Let $\phi_n : \mathcal{H} \rightarrow [0, \infty)$ ($\forall n \in \mathbb{N}$) be a sequence of continuous convex functions and $K \subset \mathcal{H}$ a nonempty closed convex set. For an arbitrarily given $\mathbf{u}_0 \in K$, the sequence $\{\mathbf{u}_n\}_{n \in \mathbb{N}} \subset K$ generated by the adaptive projected subgradient method:

$$\mathbf{u}_{n+1} = \begin{cases} P_K \left(\mathbf{u}_n - \mu_n \frac{\phi_n(\mathbf{u}_n)}{\|\phi'_n(\mathbf{u}_n)\|^2} \phi'_n(\mathbf{u}_n) \right), & \text{if } \phi'_n(\mathbf{u}_n) \neq 0, \\ \mathbf{u}_n, & \text{otherwise,} \end{cases} \quad (50)$$

where $\phi'_n(\mathbf{u}_n) \in \partial\phi_n(\mathbf{u}_n)$ and $0 \leq \mu_n \leq 2$, satisfies the following.

(*Monotome approximation*) Suppose

$$\mathbf{u}_n \notin \Omega_n := \{\mathbf{u} \in K \mid \phi_n(\mathbf{u}) = \phi_n^* := \inf_{\mathbf{v} \in K} \phi_n(\mathbf{v})\} \neq \emptyset. \quad (51)$$

Then, by using $\forall \mu_n \in \left(0, 2\left(1 - \frac{\phi_n^*}{\phi_n(\mathbf{u}_n)}\right)\right)$, we have $\|\mathbf{u}_{n+1} - \mathbf{u}_{(n)}^*\| < \|\mathbf{u}_n - \mathbf{u}_{(n)}^*\|$ for all $\mathbf{u}_{(n)} \in \Omega_n$.

(*Asymptotic optimality*) Suppose

$$\exists N_0 \in \mathbb{N} \text{ s.t. } \phi_n^* = 0 \quad \forall n \geq N_0 \quad \text{and} \quad \Omega := \bigcap_{n \geq N_0} \Omega_n \neq \emptyset. \quad (52)$$

Then, $\{\mathbf{u}_n\}_{n \in \mathbb{N}}$ is bounded. Moreover, if we specially use $\forall \mu_n \in [\epsilon_1, 2 - \epsilon_2] \subset (0, 2)$, we have $\lim_{n \rightarrow \infty} \phi_n(\mathbf{u}_n) = 0$ provided that $\{\phi'_n(\mathbf{u}_n)\}_{n \in \mathbb{N}}$ is bounded.

(*Strong convergence*) Assume (52) and Ω has some relative interior w.r.t. a hyperplane $\Pi (\subset \mathcal{H})$; i.e., there exist $\tilde{\mathbf{u}} \in \Pi \cap \Omega$ and $\exists \epsilon > 0$ satisfying $\{\mathbf{u} \in \Pi \text{ s.t. } \|\mathbf{u} - \tilde{\mathbf{u}}\| \leq \epsilon\} \subset \Omega$. Then, by using $\forall \mu_n \in [\epsilon_1, 2 - \epsilon_2] \subset (0, 2)$, $\{\mathbf{u}_n\}_{n \in \mathbb{N}}$ converges strongly to some $\hat{\mathbf{u}} \in K$, i.e., $\lim_{n \rightarrow \infty} \|\mathbf{u}_n - \hat{\mathbf{u}}\| = 0$. Moreover, $\lim_{n \rightarrow \infty} \phi_n(\hat{\mathbf{u}}) = 0$ if $\{\phi'_n(\mathbf{u}_n)\}_{n \in \mathbb{N}}$ is bounded and if there exists bounded $\{\phi'_n(\hat{\mathbf{u}})\}_{n \in \mathbb{N}}$ where $\phi'_n(\hat{\mathbf{u}}) \in \partial\phi_n(\hat{\mathbf{u}})$, $\forall n \in \mathbb{N}$.

Note that the update rule in (50) is a composite projection composed of the subgradient-based projection relative to ϕ_n and the metric projection onto K . In fact, the first projection is not the subgradient projection exactly since the step size parameter μ_n does not need to be one. This projection can be rewritten as

$$\hat{T}_{\mu_n}(\mathbf{u}_n) := \mathbf{u}_n - \mu_n \frac{\phi_n(\mathbf{u}_n)}{\|\phi'_n(\mathbf{u}_n)\|^2} \phi'_n(\mathbf{u}_n) = [(1 - \mu_n)I + \mu_n T_{sp(\phi_n)}](\mathbf{u}_n), \quad (53)$$

where I is the identity mapping. When $\mu_n = 1$, $\hat{T}_{\mu_n} = T_{sp(\phi_n)}$. When $\mu_n < 1$, the projection moves the original point towards the exact subgradient projection point, but not fully. When $\mu_n > 1$, on the other hand, the projection moves the original point beyond the exact subgradient projection point. For any $\mu_n \in (0, 2)$, \hat{T}_{μ_n} is called a μ_n -averaged quasi-nonexpansive mapping, and the properties of this mapping play

an important role in the proof of Theorem 5. The major difference of the subgradient projection method from the simple gradient method without normalization is that we know the exact range of the step size parameter μ_n for convergence because of the proper normalization of the subgradient in the subgradient projection. (See (49) and (50).) The above result is general and can be applied to many constrained optimization problems. Consider the simple case with a fixed cost function (i.e., $\phi_n(\mathbf{u}) \equiv \phi(\mathbf{u}) \ \forall n$) of which minimum is achieved in K . Let $\phi^* = \min_{\mathbf{u} \in K} \phi(\mathbf{u})$. Then, we can define $\tilde{\phi}(\mathbf{u}) := \phi(\mathbf{u}) - \phi^*$. Then, the condition (52) is trivially satisfied, and we have $\lim_{n \rightarrow \infty} \tilde{\phi}(\mathbf{u}_n) = 0$, i.e., $\lim_{n \rightarrow \infty} \phi(\mathbf{u}_n) = \phi^*$. In this case, the result reduces to the Polyak's projected subgradient method for which he showed the weak convergence [14, Theorem 1]. (For the proof of Theorem 5, refer to [16]. For the introduction of related projections, see [21].)

B. Joint Source and Relay Filter Design via the Projected Subgradient Method

Even under the LTI formulation (17, 19, 20, 21), the search space for source and relay filters $T(z)$ and $H(z)$ has countably infinite dimensions since both $T(z)$ and $H(z)$ can be IIR filters. To avoid the difficulties in searching in an infinite dimensional space and in imposing the stability condition, we restrict ourselves to the case that both $T(z)$ and $H(z)$ have FIRs as in most practical filtering applications. Then, the stability and causality constraints are automatically satisfied. In this case, the source and relay filter responses are respectively given by

$$T(z) = t_0 + t_1 z^{-1} + \dots + t_{L_s-1} z^{-L_s+1}, \quad \text{and} \quad (54)$$

$$H(z) = h_0 + h_1 z^{-1} + \dots + h_{L_r-1} z^{-L_r+1}, \quad (55)$$

where L_s and L_r are the orders of source and relay filters, respectively. Although the channel responses $H_{sr}(z)$, $H_{rd}(z)$ and $H_{sd}(z)$ do not need to have finite durations, we also assume that these channel responses have finite duration L for simplicity. For notational convenience, we define the following:

$$\mathbf{w}_m(\omega) := [1, e^{j\omega}, e^{j2\omega}, \dots, e^{j(m-1)\omega}]^T, \quad (56)$$

$$\mathbf{t} := [t_0, t_1, \dots, t_{L_s-1}]^T \in \mathbb{R}^{L_s \times 1}, \quad (57)$$

$$\mathbf{h} := [h_0, h_1, \dots, h_{L_r-1}]^T \in \mathbb{R}^{L_r \times 1}, \quad (58)$$

$$\mathbf{u} := [\mathbf{t}^T, \mathbf{h}^T]^T \in \mathbb{R}^{(L_s+L_r) \times 1}, \quad (59)$$

$$\mathbf{h}_{ab} := [h_{ab}[0], h_{ab}[1], \dots, h_{ab}[L-1]]^T \text{ for } (a, b) = (s, r), (r, d) \text{ and } (s, d). \quad (60)$$

Then, we have

$$T(e^{j\omega}) = \mathbf{w}_{L_s}^H(\omega)\mathbf{t}, \quad H(e^{j\omega}) = \mathbf{w}_{L_r}^H(\omega)\mathbf{h}, \quad H_{ab}(e^{j\omega}) = \mathbf{w}_L^H(\omega)\mathbf{h}_{ab}. \quad (61)$$

Here, we assume that \mathbf{t} and \mathbf{h} are real vectors for simplicity, but the extension to the complex case is straightforward. Now from (17) we define the cost function as

$$\phi(\mathbf{u}) = -\frac{1}{2\pi} \int_{-\pi}^{\pi} \frac{1}{2} \log_2 \left(1 + \frac{|H_{sd}(e^{j\omega}) + H_{sr}(e^{j\omega})H(e^{j\omega}; \mathbf{h})H_{rd}(e^{j\omega})|^2}{\sigma^2(|H_{rd}(e^{j\omega})H(e^{j\omega}; \mathbf{h})|^2 + 1)} |T(e^{j\omega}; \mathbf{t})|^2 \right) d\omega, \quad (62)$$

where the respective dependence of $H(e^{j\omega})$ and $T(e^{j\omega})$ on \mathbf{h} and \mathbf{t} is explicitly shown. The gradient $\phi'(\mathbf{u})$ at \mathbf{u} can be obtained after some computation as

$$\phi'(\mathbf{u}) = \frac{1}{2\pi} \int_{-\pi}^{\pi} \frac{1}{2 \ln 2} \cdot \frac{1}{1 + A(\omega)} \begin{pmatrix} B(\omega) \\ C_1(\omega)(C_2(\omega) - C_3(\omega)C_4(\omega)) \end{pmatrix} d\omega, \quad (63)$$

where $A(\omega) = \text{CNR}(e^{j\omega}; \mathbf{h}) \cdot \mathbf{t}^T \mathbf{w}_{L_s} \mathbf{w}_{L_s}^H \mathbf{t}$, $B(\omega) = \text{CNR}(e^{j\omega}; \mathbf{h}) \cdot (\mathbf{w}_{L_s} \mathbf{w}_{L_s}^H + \mathbf{w}_{L_s}^* \mathbf{w}_{L_s}^T) \mathbf{t}$, $C_1(\omega) = \mathbf{t}^T \mathbf{w}_{L_s} \mathbf{w}_{L_s}^H \mathbf{t} / D(e^{j\omega}; \mathbf{h})$, $C_2(\omega) = \nabla_{\mathbf{h}} N(e^{j\omega}; \mathbf{h})$, $C_3(\omega) = \nabla_{\mathbf{h}} D(e^{j\omega}; \mathbf{h})$ and $C_4(\omega) = \text{CNR}(e^{j\omega}; \mathbf{h})$; and $N(e^{j\omega}; \mathbf{h})$ and $D(e^{j\omega}; \mathbf{h})$ are the numerator and denominator of $\text{CNR}(e^{j\omega}; \mathbf{h})$, respectively. The source power constraint (19) is given in terms of \mathbf{t} and \mathbf{h} by

$$\frac{1}{2\pi} \int_{-\pi}^{\pi} |T(e^{j\omega})|^2 d\omega = \sum_{l=0}^{L_s-1} t_l^2 = \|\mathbf{t}\|^2 \leq P_s \quad (64)$$

by Parseval's theorem, and the constraint set for \mathbf{t} determined by (64) is simply a ball in \mathbf{t} , denoted by $B_{\mathbf{t}}(P_s)$, with no constraint on \mathbf{h} . Next, consider the power constraint at the relay. The relay power constraint (20) is expressed in terms of \mathbf{t} and \mathbf{h} as

$$\begin{aligned} & \frac{1}{2\pi} \int_{-\pi}^{\pi} |H(e^{j\omega})|^2 (|H_{sr}(e^{j\omega})|^2 \cdot |T(e^{j\omega})|^2 + \sigma^2) d\omega \\ &= \frac{1}{2\pi} \int_{-\pi}^{\pi} \mathbf{h}^T \mathbf{w}_{L_r}(\omega) \mathbf{w}_{L_r}^H(\omega) \mathbf{h} \cdot \underbrace{(|H_{sr}(e^{j\omega})|^2 \mathbf{t}^T \mathbf{w}_{L_s}(\omega) \mathbf{w}_{L_s}^H(\omega) \mathbf{t} + \sigma^2)}_{=:g(\omega; \mathbf{t})} d\omega, \\ &= \mathbf{h}^T \left(\frac{1}{2\pi} \int_{-\pi}^{\pi} g(\omega; \mathbf{t}) \mathbf{w}_{L_r}(\omega) \mathbf{w}_{L_r}^H(\omega) d\omega \right) \mathbf{h} \leq P_r. \end{aligned} \quad (65)$$

$$= \mathbf{h}^T \left(\frac{1}{2\pi} \int_{-\pi}^{\pi} g(\omega; \mathbf{t}) \mathbf{w}_{L_r}(\omega) \mathbf{w}_{L_r}^H(\omega) d\omega \right) \mathbf{h} \leq P_r. \quad (66)$$

Note that the constraint set for (\mathbf{t}, \mathbf{h}) determined by (66) is bi-convex, i.e., convex in each of \mathbf{t} and \mathbf{h} but not jointly convex. The constraint set for \mathbf{h} for a given \mathbf{t} is an ellipsoid, as shown in (66). Let us denote this ellipsoid by $\xi_{\mathbf{h}}(\mathbf{t})$. The above inequality can also be written as

$$\begin{aligned} & \mathbf{t}^T \left(\frac{1}{2\pi} \int_{-\pi}^{\pi} (|H_{sr}(e^{j\omega})|^2 \mathbf{h}^T \mathbf{w}_{L_r}(\omega) \mathbf{w}_{L_r}^H(\omega) \mathbf{h}) \mathbf{w}_{L_s}(\omega) \mathbf{w}_{L_s}^H(\omega) d\omega \right) \mathbf{t} \\ & \quad + \frac{\sigma^2}{2\pi} \int_{-\pi}^{\pi} \mathbf{h}^T \mathbf{w}_{L_r}(\omega) \mathbf{w}_{L_r}^H(\omega) \mathbf{h} d\omega \leq P_r, \end{aligned} \quad (67)$$

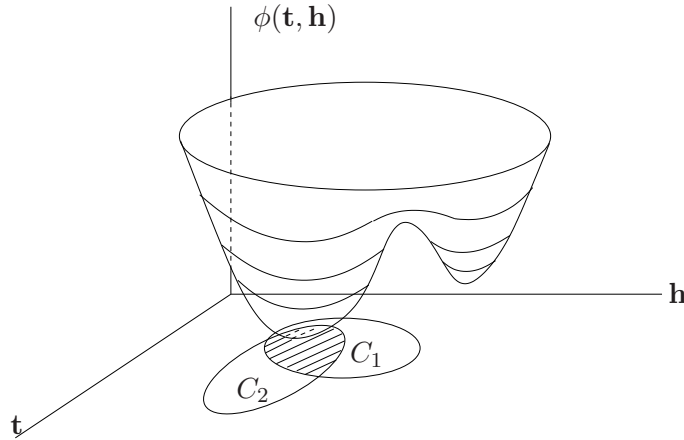


Fig. 7

COST MINIMIZATION OVER THE INTERSECTION OF TWO CONSTRAINT SETS

and, therefore, the constraint set for \mathbf{t} for a given \mathbf{h} is also an ellipsoid.

Now, the problem under the LTI FIR formulation is given by

$$\min_{\mathbf{t}, \mathbf{h}} \phi(\mathbf{t}, \mathbf{h}) \tag{68}$$

such that

$$(\mathbf{t}, \mathbf{h}) \in C_1 \text{ and } (\mathbf{t}, \mathbf{h}) \in C_2, \tag{69}$$

where $\phi(\mathbf{t}, \mathbf{h})$ is given by (62), and C_1 and C_2 are the constraint sets determined by (64) and (66), respectively. The situation is depicted in Fig. 7. Even though $\phi(\mathbf{t}, \mathbf{h})$ is not jointly convex in \mathbf{t} and \mathbf{h} , we can still apply the projected subgradient method in Theorem 5. Suppose now that $K := C_1 \cap C_2$ is convex. Then, applying the projected subgradient method (50) with $\mathbf{u}_0 \in K$ leads to the convergence to a local minimum at least. Due to the nonconvexity of C_2 , however, K is not a convex set. To circumvent this issue, let us investigate the structure of the two constraint sets further. Fig. 8 shows the two constraint sets, C_1 and C_2 , and their intersection K in the case of $\mathbf{t} = (t_0, t_1)$ and $\mathbf{h} = h_0$. C_1 and C_2 are the red cylinder and the blue shape that looks like a mountain on one side and is symmetric about the $h_0 = 0$ plane in the left side of Fig. 8, respectively. In this case, the ellipsoid $\xi_{\mathbf{h}}(\mathbf{t}')$ is a line segment passing through $(\mathbf{t}', 0)$ ending at the upper and the lower surfaces of the blue shape, as shown in Fig. 8. As mentioned already, for a given \mathbf{h} the constraint set for \mathbf{t} is an ellipsoid. (See (67).) So, we have an ellipsoidal cut of the blue shape by a plane perpendicular to the h_0 -axis. Thus, $C_1 \cap C_2$ is given by the shape in the right side of Fig. 8, which looks like a cylinder with bulges on the top and the bottom. If we are willing to sacrifice the bulging regions from the feasibility set, we can construct a convex set $\tilde{K} \subset K$

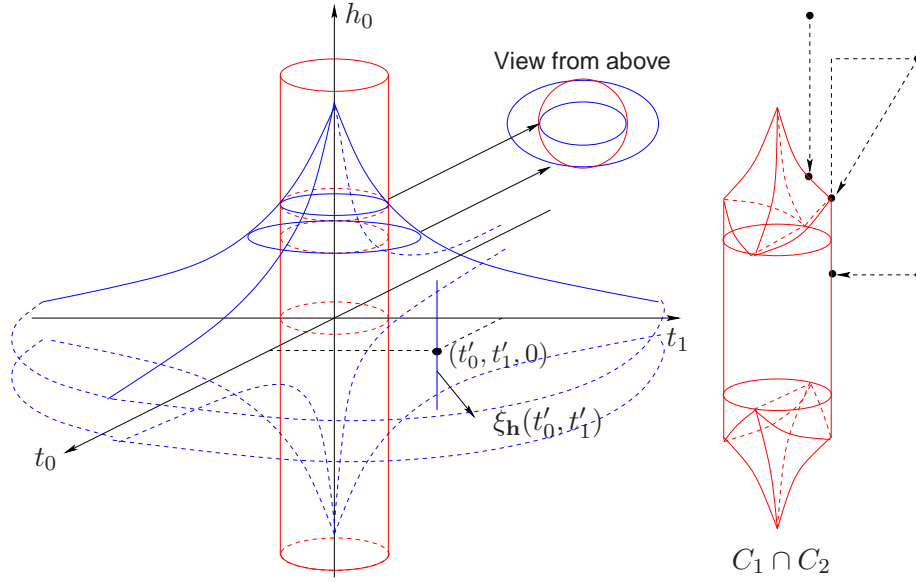


Fig. 8

THE STRUCTURE OF TWO CONSTRAINT SETS IN CASE OF $\mathbf{t} = (t_0, t_1)$ AND $\mathbf{h} = h_0$

as the Cartesian product of $B_{\mathbf{t}}(P_s)$ and $\Xi_{\mathbf{h}}(P_s, P_r)$, i.e.,

$$\tilde{K} := B_{\mathbf{t}}(P_s) \times \Xi_{\mathbf{h}}(P_s, P_r), \quad (70)$$

where

$$\Xi_{\mathbf{h}}(P_s, P_r) = \bigcap_{\mathbf{t} \in B_{\mathbf{t}}(P_s)} \xi_{\mathbf{h}}(\mathbf{t}) = \bigcap_{\mathbf{t} \in \text{surface}(B_{\mathbf{t}}(P_s))} \xi_{\mathbf{h}}(\mathbf{t}). \quad (71)$$

The second equality in (71) is because $\xi_{\mathbf{h}}(\mathbf{t}') \subset \xi_{\mathbf{h}}(\gamma\mathbf{t}')$ for $\gamma \in [0, 1]$. This can easily be verified from (65). For $\gamma\mathbf{t}'$, $|T(e^{j\omega})|^2$ will simply scale down to $\gamma^2|T(e^{j\omega})|^2$, and $|H(e^{j\omega})|^2$ satisfying the inequality with $|T(e^{j\omega})|^2$ will satisfy the inequality with $\gamma^2|T(e^{j\omega})|^2$. Here, $\Xi_{\mathbf{h}}(P_s, P_r)$ is convex since it is the intersection of ellipsoids. Also, \tilde{K} is convex due to its Cartesian product structure. In the considered case of (t_0, t_1, h_0) , \tilde{K} is exactly the red cylinder in the right side of Fig. 8. Based on the above discussion, we now provide our first algorithm for the joint source and relay filter design.

Algorithm 1: • Initialization: Set \mathbf{u}_0 properly, e.g.,

$$\mathbf{u}_0 = [\mathbf{t}_0^T, \mathbf{0}^T]^T \quad (72)$$

with $\mathbf{t}_0 = [\sqrt{\frac{P_s}{L_s}}[1, 1, \dots, 1]^T$. (It is easy to verify that this $\mathbf{u}_0 \in \tilde{K} \subset K$.)

- Update:

$$\mathbf{u}_{n+1} = \begin{cases} P_{\tilde{K}} \left(\mathbf{u}_n - \mu_n \frac{\phi_n(\mathbf{u}_n)}{\|\phi'_n(\mathbf{u}_n)\|^2} \phi'_n(\mathbf{u}_n) \right), & \text{if } \phi'_n(\mathbf{u}_n) \neq 0, \\ \mathbf{u}_n, & \text{otherwise,} \end{cases} \quad (73)$$

where $\phi(\mathbf{u})$ and $\phi'(\mathbf{u})$ are given by (62) and (63), respectively, $0 < \mu_n < 2$ and $\mathbf{u}_n = [\mathbf{t}_n^T, \mathbf{h}_n^T]^T$.

- Stopping rule: Stop the update either when \mathbf{u}_n does not change further or when the number of iterations exceeds a preset maximum.

Due to the Cartesian product structure of \tilde{K} in (70), the metric projection $P_{\tilde{K}}$ can be implemented by the composition of two separate projections, one in \mathbf{t} projecting onto $B_{\mathbf{t}}(P_s)$ and then the other in \mathbf{h} projecting onto $\Xi_{\mathbf{h}}(P_s, P_t)$, i.e.,

$$P_{\tilde{K}} = P_{\Xi_{\mathbf{h}}(P_s, P_t)} \circ P_{B_{\mathbf{t}}(P_s)}, \quad (74)$$

where the projection onto a ball is simply given by

$$P_{B_{\mathbf{t}}(P_s)}(\mathbf{t}) = \begin{cases} \mathbf{t}, & \text{if } \|\mathbf{t}\|^2 \leq P_s, \\ \frac{\sqrt{P_s} \mathbf{t}}{\|\mathbf{t}\|}, & \text{otherwise,} \end{cases} \quad (75)$$

and $P_{\Xi_{\mathbf{h}}(P_s, P_t)}$ can be approximated by using the successive projection method [22]. That is, we uniformly partition the surface of the L_s -dimensional ball with radius $\sqrt{P_s}$ into M subsets, and select the center \mathbf{t}_m of subset m . Then, $\Xi_{\mathbf{h}}(P_s, P_t) \approx \cap_{m=1}^M \xi_{\mathbf{h}}(\mathbf{t}_m)$ and

$$P_{\Xi_{\mathbf{h}}(P_s, P_t)}(\mathbf{h}) \approx P_{\xi_{\mathbf{h}}(\mathbf{t}_M)} \circ P_{\xi_{\mathbf{h}}(\mathbf{t}_{M-1})} \circ \cdots \circ P_{\xi_{\mathbf{h}}(\mathbf{t}_1)}(\mathbf{h}), \quad (76)$$

where the projection onto an ellipsoid can easily be implemented by a known method like the one in [23]. If $\phi'(\mathbf{u}) \neq 0$ for all $\mathbf{u} \in \tilde{K}$, then Algorithm 1 will find the point that yields the maximum rate within \tilde{K} . Otherwise, Algorithm 1 finds a local optimum attracting \mathbf{u}_0 , and convergence is guaranteed. However, the complexity of the projection $P_{\Xi_{\mathbf{h}}(P_s, P_t)}(\mathbf{h})$ is prohibitive even for small values of L_s . Thus, we propose a simplified algorithm to eliminate this difficulty in the following.

Algorithm 2: • Initialization of \mathbf{u}_0 .

- Update:

$$\mathbf{u}_{n+1} = \begin{cases} P_{\xi_{\mathbf{h}}(P_{B_{\mathbf{t}}(P_s)}(\mathbf{t}_n))}(\mathbf{h}_n) \circ P_{B_{\mathbf{t}}(P_s)}(\mathbf{t}_n) \circ \left(\mathbf{u}_n - \mu_n \frac{\phi_n(\mathbf{u}_n)}{\|\phi'_n(\mathbf{u}_n)\|^2} \phi'_n(\mathbf{u}_n) \right), & \text{if } \phi'_n(\mathbf{u}_n) \neq 0, \\ \mathbf{u}_n, & \text{otherwise.} \end{cases} \quad (77)$$

- Stopping rule: The same as that in Algorithm 1.

In the initialization step, we can consider other initial points than the example in Algorithm 1. For example,

$$\mathbf{t}_0 = [\sqrt{P_s}, 0, \dots, 0]^T \text{ and } \mathbf{h}_0 = P_{\xi_{\mathbf{h}}(\mathbf{t}_0)}([1, \dots, 1]^T). \quad (78)$$

With such an initial point, we can start the algorithm from the full power use at the relay. In Algorithm 2, the subgradient projection is the same as that in Algorithm 1, but the projection to K is now different. Here, we first project only the \mathbf{t}_n coordinates to the ball $B_{\mathbf{t}}(P_s)$, and then project the \mathbf{h}_n coordinates onto the \mathbf{h} -ellipsoid $\xi_{\mathbf{h}}(P_{B_{\mathbf{t}}(P_s)}(\mathbf{t}_n))$ corresponding to $P_{B_{\mathbf{t}}(P_s)}(\mathbf{t}_n)$ given by (66); several projection examples in the case of $L_s = 2$ and $L_r = 1$ are shown in the right side of Fig. 8. In this way, the metric projection to K is approximated and highly simplified, and $\mathbf{u}_n \in K$ for all n . The convergence of Algorithm 2 is not guaranteed theoretically, but there is no loss in the feasibility set in this case. It is observed numerically that Algorithm 2 is stable and works well. This is because K seems almost convex as seen in the example in Fig. 8, and the proposed two-step projection onto K approximates the metric projection onto K well due to the almost cylindrical structure of K except the top and bottom. Under our formulation, it is straightforward to impose the strict causality constraint on the relay filter $H(z)$ that captures the possible delay at the relay for digital processing; simply remove h_0 in (55) and follow the same procedure as the causal case.

VI. NUMERICAL RESULTS

To evaluate the performance of the proposed joint filter design method presented in Section V, we ran extensive simulations under various channel conditions. The channel order L of all the propagation channels $H_{sr}(z)$, $H_{rd}(z)$ and $H_{sd}(z)$ was selected as $L = 5$, and each channel tap coefficient was generated independently and identically-distributedly (i.i.d.) according to a Rayleigh distribution with a different variance for a different channel, i.e.,

$$h_{sd}[l] \stackrel{i.i.d.}{\sim} \mathcal{N}(0, \sigma_{sd}^2), \quad h_{sr}[l] \stackrel{i.i.d.}{\sim} \mathcal{N}(0, \sigma_{sr}^2) \quad \text{and} \quad h_{rd}[l] \stackrel{i.i.d.}{\sim} \mathcal{N}(0, \sigma_{rd}^2) \quad (79)$$

for $l = 0, 1, \dots, L - 1$. Throughout the simulations, we fixed $\sigma^2 = 1$ and used $L_s = 30$ and $L_r = 20$ for the orders of the source and relay filters, respectively, to allow enough freedom for the two filters considering $L = 5$. We used Algorithm 2 with the initial point** (78) for the simulations, and the step size for the algorithm was adaptively changed according to $\mu_n = 1/\sqrt{n}$ as the number of iterations increases. The stopping condition for the algorithm was either that the square of the normalized difference of two

**We observed that Algorithm 2 with the initialization (72) did not make a noticeable difference.

successive updates is less than 10^{-5} (i.e., $\|\mathbf{u}_{n+1} - \mathbf{u}_n\|^2 / \|\mathbf{u}_n\|^2 \leq 10^{-5}$) or that the number of iterations exceeds 1000. For the numerical integration to compute the quantities (62, 63, 66), we used a 512-point Gaussian quadrature method over $[-\pi, \pi]$. Since it is not clear how to optimally apply the known coding strategies such as DF and CF to the case of ISI channels, we do not consider these schemes in this section, and thus we use the AF scheme as the performance reference.

First, Fig. 9 shows the frequency responses related to the proposed method. The channel coefficients for this figure were generated randomly according to $\sigma_{sr}^2 = \sigma_{rd}^2 = \sigma_{sd}^2 = 1$ and given by $H_{sr} = 1.8833 + 0.3254z^{-1} - 0.0952z^{-2} + 0.0312z^3 - 0.6138z^{-4}$, $H_{rd} = -0.0728 + 1.3148z^{-1} + 0.9783z^{-2} + 1.7221z^3 - 0.4123z^{-4}$ and $H_{sd} = -0.8864 - 1.8402z^{-1} - 1.6282z^{-2} - 1.1738z^3 - 0.4154z^{-4}$. $P_s = P_r = 1$. The flat^{††} dashed line represents the input spectrum of the conventional AF scheme, and the dotted line is the inverse of the CNR density, i.e., the effect noise level, in the case that the AF scheme is used at the relay. It is seen that there are two peaks in the noise level for the AF scheme around the normalized frequency values of 0.6 and 1. Note that the peak around 0.6 is very high and its width is also large, whereas the peak around 1 is mild. Now the red solid line marked with + denotes the effective noise level generated by the relay filter designed by the proposed method. We recognize that the designed relay filter is smart. One could imagine that a reasonable relay filter would suppress the frequency band having a bad overall response with the AF scheme and enhance the frequency band having a good overall response with the AF scheme so that the water-filling by the source filter might be enhanced. This is exactly the case with the mild noise peak around 1; the designed relay filter reinforces the mild noise peak. However, the designed relay filter suppresses the severe noise peak with a large width around 0.6 instead of reinforcing it. This is because the width of the severe peak is large and, thus, the loss of this frequency band will reduce the transmission rate. To this optimally shaped noise level, the water-filling-type source power allocation is performed by the designed source filter satisfying both the source and relay power constraints jointly with the designed relay filter; for the frequency bands around the two noise peaks the power is not allocated, as seen in the figure. (See the green solid line without any markers.) Similar behaviors are observed in other settings even though they are not shown in this paper.

^{††}The reason why the flat input spectrum is used for the conventional AF scheme is that even for a given relay filter, e.g., the AF filter, the optimal power allocation to maximize the transmission rate (17) not only with the source power constraint (19) but also with the relay power constraint (20) in ISI channels is not a trivial problem; this is not a simple and known water-filling problem with a single total power constraint because of the term $|H_{sr}(e^{j\omega})|^2$ in (20) unless $H_{sr}(e^{j\omega})$ is constant over $[-\pi, \pi]$. As far as we know, this problem was not handled before, and the two-step projection method in this paper provides one way to accomplish this in general ISI channels.

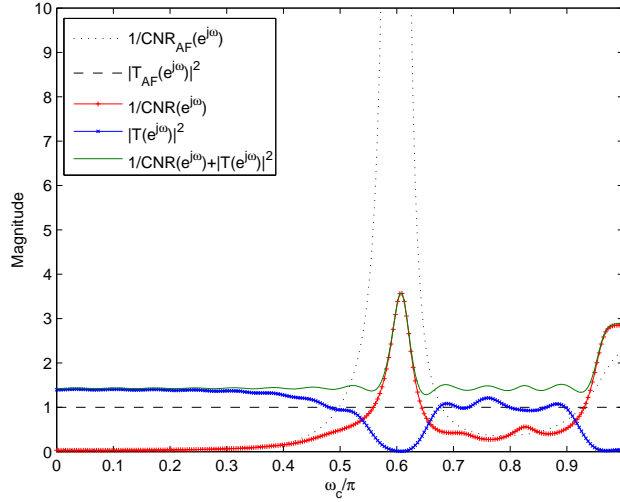


Fig. 9

THE FREQUENCY RESPONSES RELATED TO THE PROPOSED METHOD

Next, let us see the performance of the proposed method in various channel settings. Fig. 10 shows the transmission rate achieved by the proposed method averaged over 100 independent channel realizations for each of the different channel gain settings when $P_s = P_r$. We considered both causal and strictly causal filtering for the proposed method. For the strictly causal filtering, we eliminated the t_0 and h_0 terms in the formulation and kept the same filter orders L_s and L_r as those in the causal filtering case. We considered two sets of channel conditions; in one set the direct S-D link has a reasonable strength compared with the S-R and R-D links (Fig. 10 (a), (b), (c), (d)), and in the other set the direct link is weak compared with the S-R and R-D links (Fig. 10 (e) and (f)). (We did not consider the case that the direct link is stronger than the S-R and R-D links since it is unnecessary to use the relay in this case.) It is seen in Fig. 10 that the gain obtained by the proposed joint source and relay filtering over the AF scheme is noticeable. In particular, Fig. 10 (c) shows the performance when $P_s = P_r$, $\sigma^2 = 1$, $\sigma_{sd}^2 = 1$, $\sigma_{sr}^2 = 1$ and $\sigma_{rd}^2 = 4$, which is equivalent to the flat-fading case of $a = 1$ and $b = 2$ in Fig. 3 (a) and (b) and Fig. 5. Compared with the flat-fading case shown in Fig. 5 (c), the gain by the proposed joint design over the AF scheme in ISI channels is significant. It is also seen that the loss caused by the strict causality of filtering is not significant in the proposed scheme. This is because removing one tap out of 30 or 20 taps does not reduce the degree of freedom of the filters much. Fig. 10 (e) and (f) show the case that the direct link is weak compared with the S-R and R-D

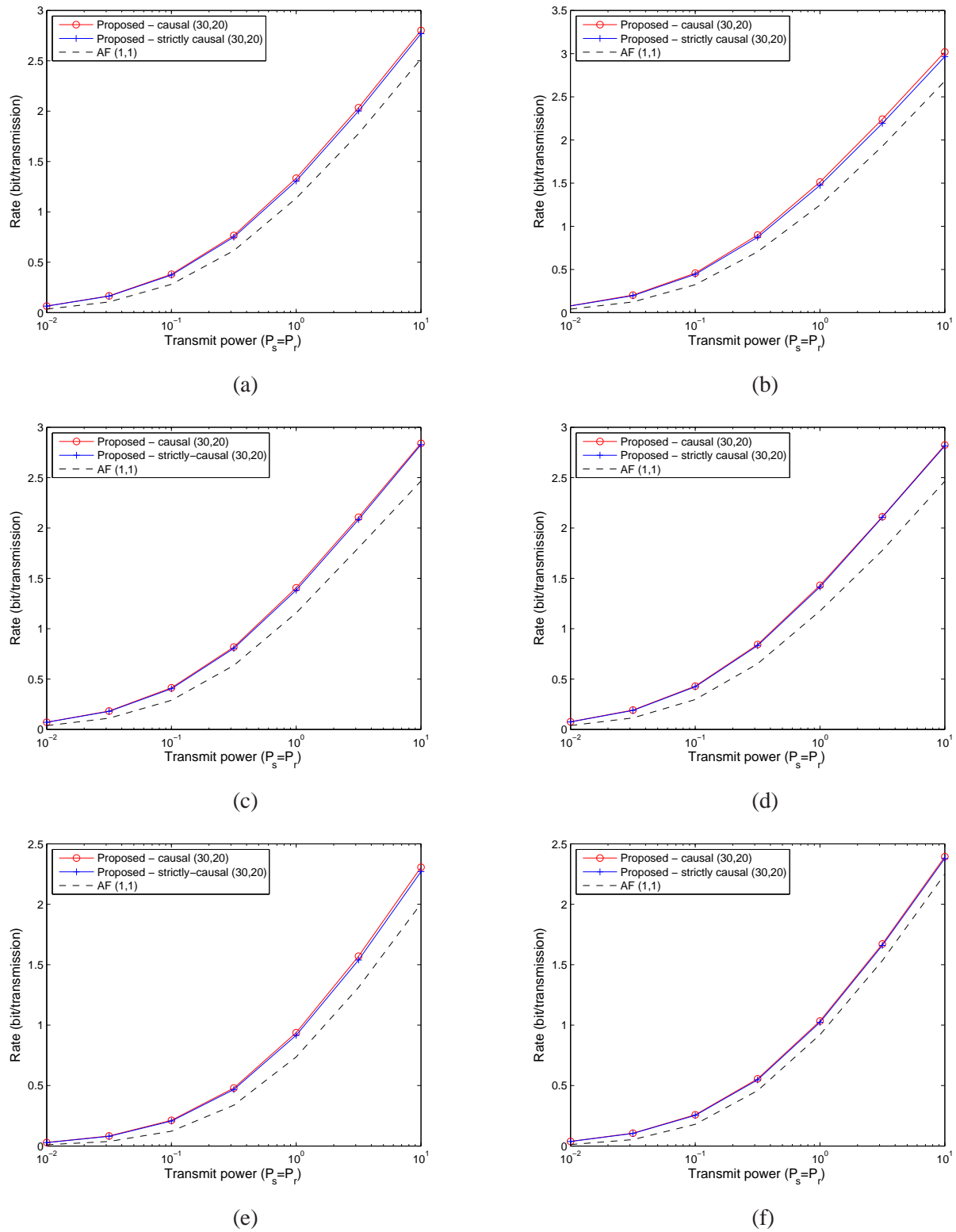


Fig. 10

TRANSMISSION RATE AVERAGED OVER CHANNEL REALIZATIONS ($P_s = P_r$): (A) $\sigma_{sd}^2 = 1, \sigma_{sr}^2 = 1, \sigma_{rd}^2 = 1$,
 (B) $\sigma_{sd}^2 = 1, \sigma_{sr}^2 = 4, \sigma_{rd}^2 = 1$, (C) $\sigma_{sd}^2 = 1, \sigma_{sr}^2 = 1, \sigma_{rd}^2 = 4$, (D) $\sigma_{sd}^2 = 1, \sigma_{sr}^2 = 1, \sigma_{rd}^2 = 10$, (E) $\sigma_{sd}^2 = 1/4$,
 September 19, 2018 $\sigma_{sr}^2 = 1, \sigma_{rd}^2 = 1$, AND (F) $\sigma_{sd}^2 = 1/10, \sigma_{sr}^2 = 1, \sigma_{rd}^2 = 10$ DRAFT

links. Similar results are seen in the figure. Fig. 10 (f) shows the smallest gain among the six cases. This is explained as follows. As seen in (17, 18), the gain of the joint filtering depends on various factors. The worst situation for the performance of the joint filtering is the case that $H_{sd}(e^{j\omega}) \approx 0$ and $H_{rd}(e^{j\omega}) \gg 0$ such that $|H_{rd}(e^{j\omega})H(e^{j\omega})| \gg 1$. In this case, the CNR density in (18) is approximated by $CNR(e^{j\omega}) \approx |H_{sr}(e^{j\omega})H(e^{j\omega})H_{rd}(e^{j\omega})|^2 / (\sigma^2 |H_{rd}(e^{j\omega})H(e^{j\omega})|^2) = |H_{sr}(e^{j\omega})|^2 / \sigma^2$; and thus the impact of the relay filter disappears and only the optimal power allocation by the source filter under the two power constraints is effective. Even in this case, a non-negligible gain is observed. Although the results in the cases of $P_s = 2P_r$ and $2P_s = P_r$ are not shown in this paper, we observed similar results to the case of $P_s = P_r$.

VII. CONCLUSIONS

We have considered the linear Gaussian relay problem. By adopting the LTI relay filtering and realizable input spectra, we have converted the problem to a joint design problem of source and relay filters. We have investigated the performance of this joint LTI filtering in flat-fading relay channels, and have shown the optimality of the AF scheme within the class of one-tap filters. In general ISI relay channels, we have developed a practical method for the joint filter design to maximize the transmission rate based on the projected subgradient method under the LTI FIR filtering framework, and have shown numerically that the gain of the proposed design is noticeable compared with the AF scheme in ISI relay channels.

ACKNOWLEDGEMENT

The authors of this paper wish to thank Gilwon Lee, Masahiro Yukawa and Isao Yamada for their introduction to the (adaptive) projected subgradient method.

REFERENCES

- [1] T. M. Cover and A. El Gamal, "Capacity theorems for the relay channel," *IEEE Trans. Inf. Theory*, vol. 25, no. 9, pp. 572 – 584, Sep. 1979.
- [2] A. El Gamal and M. Aref, "The capacity of the semideterministic relay channel," *IEEE Trans. Inf. Theory*, vol. 28, no. 3, pp. 536, May 1986.
- [3] S. Zahedi, M. Mohseni and A. El Gamal, "On the capacity of AWGN relay channels with linear relaying functions," in *Proc. ISIT*, 2004.
- [4] A. El Gamal, M. Mohseni and S. Zahedi, "Bounds on capacity and minimum energy-per-bit for AWGN relay channels," *IEEE Trans. Inf. Theory*, vol. 52, no. 4, pp. 1545 – 1561, Apr. 2006.
- [5] G. Kramer, M. Gastpar and P. Gupta, "Cooperative strategies and capacity theorems for relay networks," *IEEE Trans. Inf. Theory*, vol. 51, no. 9, pp. 3037 – 3063, Sep. 2005.
- [6] A. El Gamal, N. Hassanpour and J. Mammen, "Relay networks with delays," *IEEE Trans. Inf. Theory*, vol. 53, no. 10, pp. 3413 – 3431, Oct. 2007.

- [7] A. del Coso and C. Ibars, "Achievable rates for the AWGN channel with multiple parallel relays," *IEEE Trans. Wireless Commun.*, vol. 8, no. 5, pp. 2524 – 2534, May 2009.
- [8] M. N. Khormuji and M. Skoglund, "On instantaneous relaying," *IEEE Trans. Inf. Theory*, vol. 56, no. 7, pp. 3378 – 3394, Jul. 2010.
- [9] H. Chen, A. B. Gershman and S. Shahbazpanahi, "Filter-and-forward distributed beamforming in relay networks with frequency selective fading," *IEEE Trans. Signal Process.*, vol. 58, no. 3, pp. 1251 – 1262, Mar. 2010.
- [10] Y.-W. Liang, A. Ikhlef, W. Gerstacker and R. Schober, "Cooperative filter-and-forward beamforming for frequency-selective channels with equalization," *IEEE Trans. Wireless Commun.*, vol. 10, no. 1, pp. 228 – 239, Jan. 2011.
- [11] U. Grenander and G. Szegö, *Toeplitz Forms and Their Applications*, Berkeley, CA: Univ. of California Press, 1958.
- [12] P. J. Brockwell and R. A. Davis, *Time Series: Theory and Methods*, New York: 2nd Edition, Springer, 1991.
- [13] R. G. Gallager, *Information Theory and Reliable Communication*, New York, NY: Wiley, 1968.
- [14] B. T. Polyak, "Minimization of unsmooth functionals," *USSR Comput. Math. Phys.*, vol. 9, no. 1, pp. 14 – 29, 1969.
- [15] I. Yamada and N. Ogura, "Adaptive projected subgradient method for asymptotic minimization of sequence of nonnegative convex functions," *Numer. Funct. Anal. and Optimiz.*, vol. 25, no. 7 - 8, pp. 593 – 617, Jan. 2004.
- [16] K. Slavakis, I. Yamada and N. Ogura, "The adaptive projected subgradient method over the fixed point set of strongly attracting nonexpansive mappings," *Numer. Funct. Anal. and Optimiz.*, vol. 27, no. 7, pp. 905 – 930, 2006.
- [17] C.-T. Chen, *Linear System Theory and Design*, Oxford Univ. Press, New York, NY, 1999.
- [18] T. Kailath, A. H. Sayed and B. Hassibi, *Linear Estimation*, Prentice-Hall, Upper Saddle River, NJ, 2000.
- [19] T. Cover and J. Thomas, *Elements of Information Theory*, 2nd Ed., John Wiley & Sons, Inc., New York, NY, 2006.
- [20] Stephen Boyd and Lieven Vandenbergh, *Convex Optimization*, Cambridge Univ. Press, New York, NY, 2004.
- [21] S. Theodoridis, K. Slavakis and I. Yamada, "Adaptive Learning in a World of Projections," *IEEE Signal Processing Mag.*, vol. 28, no. 1, pp. 97 – 123, Jan. 2011.
- [22] Y. Censor and S. A. Zenios, *Parallel Optimization: Theory, Algorithms and Applications*, Oxford Univ. Press, New York, NY, 1997.
- [23] Yu. N. Kiseliiov, "Algorithms of projection of a point onto an ellipsoid," *Lithuanian Mathematical Journal*, vol. 34, no. 2, pp. 141 – 159, 1994.